Characterization of the Healthy Peri-implant Mucosa

Teresa Heck[1], Asfandyar Tariq Sheikh[1], Khushboo Kalani[1], Junying Li[2], Shayan Barootchi[4], I-Ching Wang[3], Hom-Lay Wang[1]

[1]Department of Periodontology and Oral Medicine, University of Michigan School of Dentistry, Ann Arbor, USA

[2]Department of Biologic and Materials Sciences & Prosthodontics, University of Michigan School of Dentistry, Ann Arbor, USA

[2]Department of Periodontics, University of Iowa, Iowa City, USA

[3]Department of Periodontology, Harvard School of Dental Medicine, Boston, USA

Correspondence

Teresa Heck, DDS

Department of Periodontics and Oral Medicine

The University of Michigan - School of Dentistry
1011 North University Avenue
48109-1078, Ann Arbor, MI - USA

Funding information

Rackham Graduate Student Research Grant of the University of Michigan, and the Delta Dental Fund Grant, Award Number: AWD021537

Asfandyar Tariq Sheikh and Khushboo Kalani contributed equally to this work.

Abstract

Objective: This cross-sectional study aimed to characterize the soft tissue around healthy implants and compare it with the soft tissue of healthy natural teeth.

Materials and Methods: A split-mouth cross-sectional study involving 66 maxillary anterior implants and teeth was conducted. Outcome measures included the following: Papilla dimensions and distance to the contact point, soft tissue thickness, Keratinized tissue (KT) width, CIELAB color values, blood flow as measured via ultrasonographic power and perfusion, buccal bone thickness, and descriptive results such as stippling, contour, form, and texture (IRB: HUM00194618).

Results: When compared to the contralateral healthy teeth, implants exhibited statistically significant differences (SSD) with regards to having thicker buccal soft tissues. Additionally, the free gingival margin of implants exhibited statistical significance in a* hue changes (along the red-green axis) in correlation with soft tissue thickness. Data suggested a linear relationship between individual CIELAB L*a*b* values and soft tissue thickness. All other outcome measures showed no statistically significant differences.

Conclusions: One of the primary findings of this study suggests that soft tissue color is influenced in a linear fashion with increasing tissue thickness, regardless of whether it is an implant or tooth site. This may have implications regarding esthetic changes after soft tissue grafting.

KEYWORDS

connective tissue biology; diagnosis; implantology; osseointegration.

Thesis submitted in partial fulfillment of the requirements for the degree of Master of Science in Periodontics from the Horace H. Rackham School of Graduate Studies at the University of Michigan, Ann Arbor, 2024.

Table of Contents

Abbreviations list

- Clinical attachment level (CAL)
- Probing depth (PD)
- Gingival recession (REC)
- Cemento-enamel junction (CEJ)
- Mesial papilla (MPAP)
- Distal papilla (DPAP)
- Crestal bone thickness (CBT)
- Distance from bone crest to CEJ (BC-CEJ)
- Keratinized tissue width (KTW)

List of Tables

TABLE 16: ΔE comparing tooth zones to each other

List of Figures

Figure 10: Linear regression analysis of scatter plot data, showing a negative relationship between implant a* value and the thickness of the supracrestal tissue adhesion.

Figure 11: Linear regression analysis of scatter plot data, showing a weakly positive relationship between tooth a* value and the thickness of the supracrestal tissue attachment.

Figure 12: Linear regression analysis of scatter plot data, showing a positive relationship between implant L* value and the thickness of the free gingival margin.

Figure 13: Linear regression analysis of scatter plot data, showing a weakly positive relationship between tooth L* value and thickness of the free gingival margin.

Figure 14: Linear regression analysis of scatter plot data, showing a positive relationship between implant L* value and thickness of the supracrestal tissue adhesion.

Figure 15: Linear regression analysis of scatter plot data, showing a very weakly negative relationship between tooth L* value and thickness of the supracrestal tissue attachment.

Figure 16: Linear regression analysis of scatter plot data, showing a negative relationship between implant b* value and thickness of the free gingival margin.

Figure 17: Linear regression analysis of scatter plot data, showing a positive relationship between tooth b* value and thickness of the free gingival margin.

Figure 18: Linear regression analysis of scatter plot data, showing a weakly negative relationship between implant b* value and thickness of the supracrestal tissue adhesion.

Figure 19: Linear regression analysis of scatter plot data, showing a weakly negative relationship between implant b* value and thickness of the supracrestal tissue adhesion.

Figure 20: Left image: Natural tooth with perfusion analysis showing vascular flow within the buccal tissues. Right image: Power analysis showing the velocity of vascular flow of the same natural tooth.

Figure 21: Photoshop-based measurements. D -CEJ: Distal papilla base (aka, “papilla width”) measured from gingival zeniths of adjacent teeth. DPAP H: Height of the distal papilla as measured from D CEJ-CEJ to the papilla tip. Similar measurement landmarks are used for M CEJ-CEJ, MPAP H height.
Figure 21: Photoshop-based measurements.

Figure 22: Clinical photo samples.

Figure 23: Papilla thickness comparison between implants and natural teeth, obtained via ultrasonographic analysis of sagittal “slice” sections in Horos software.

Figure 24: Implant exhibitingExample of an implant-supported crown surrounded by healthy peri-implant mucosal tissues at the #8 site.

Figure 24: Color measurement zones. Each zone measured 2x2 mm. From left to right: Free mucosal margin, supracrestal tissue adhesion, MGJ, mucosa apical to MGJ, mesial and distal papillae.

Figure 25: Visualization of the color averages of the different implant zones.

Figure 26: Visualization of the color averages of the different tooth zones.

Figure 27: Clinical example of an implant (#5i) surrounded by healthy periimplant mucosa.

Introduction

The healthy gingiva of teeth often expresses the following characteristics: knife-edged marginal gingiva; coral pink in color; pointed papillae filling the interproximal space; moderately scalloped contours following the underlying bone; firm; resilient with stippled surface; well demarcated mucogingival junction; no bleeding or exudate; and tightly adapting around the necks of the teeth (Gargiulo et al., 1961; Highfield, 2009). It has been suggested that the presence of a healthy gingiva is essential for preventing gingival recession and maintaining levels of connective tissue attachment (Afshar-Mohajer & Stahl, 1977). Histologically, the gingiva is attached to the tooth surface at the dento-gingival junction (Gargiulo et al., 1961), which is composed of junctional epithelium (JE), supra-crestal connective tissue (CT) fibers, and the tooth. The junctional epithelium and CT together are known as biologic width (now termed supracrestal tissue attachment (Jepsen et al., 2018), and the biologic width must remain intact or the gingiva will appear cyanotic and not heal even with best plaque control (Armitage et al., 1977).

Likewise, a variety of clinical and radiographic parameters have been identified to evaluate long-term success of implants (Albrektsson et al., 1986; Benic et al., 2012; Souza et al., 2016). These factors are: (i) the biologic width (now termed supracrestal tissue adhesion) (Jepsen et al., 2018), (ii) the papilla height and the soft-tissue level (mucosal margin) on the buccal side of the implant, (iii) the amount of soft-tissue volume, (iv) the amount of keratinized tissue, and (v) the phenotype of the mucosa.

The presence of infection or inflammation causes changes in the appearance of gingival soft tissue. Muhlemann et al. 1971 (Mühlemann & Son, 1971) indicated the clinical signs of gingival inflammation as enlarged gingival contours due to edema or fibrosis, color transition to a red or bluish-red hue, elevated sulcular temperature (Haffajee et al., 1992), bleeding on probing (BOP) (Löe & Wright, 1965), and increase in the gingival exudates. However, the intensity of the clinical signs and symptoms of gingivitis will vary between individuals (Tatakis & Trombelli, 2004). Histopathologic changes include proliferation of basal junctional epithelium leading to apical and lateral cell migration, vasculitis of blood vessels adjacent to the JE, and progressive destruction of the collagen fiber network (Highfield, 2009). Peri-implant health is identified as the absence of erythema, BOP, swelling, and suppuration. Periodontal health is defined as intact periodontium with absence of BOP, erythema, edema, and absence of clinical attachment loss and bone loss.

The color of underlying hard tissue of the natural teeth can affect the color of the gingiva. A tooth that has been endodontically treated might display blueish and grayish discoloration of the gingiva (Michalakis et al., 2004), and grayish discoloration of the gingiva could be resulted from metallic inter-radicular posts (Hunter, 1987). According to Ferrari et al. (Ferrari et al., 2017), the color of the implant abutment has no effect on the color of the mucosa that surrounds the implant, but the implant phenotype, which is the thickness of the peri-implant mucosa from the buccal side, is believed to be responsible for the soft tissue color around implants (Jung et al., 2008). Kleinhein et al. (Kleinheinz et al., 2005) suggested that the color of soft tissues around the implant is related to the thickness of the keratinized epithelium, the quantity of blood vessels, and the quality and density of the collagen fibers. Furthermore, it has been speculated that peri-implant mucosa is more translucent than

gingival tissues because of reduced vascularization (Abrahamsson et al., 1998; Jun et al., 2013).

The gingival phenotype (old name - biotype) is one of the factors related to periodontal health and treatment success. In 1969, Ochsenbein and Ross indicated that there were two main types of gingiva morphology (Ochsenbein & Ross, 1969), namely the scalloped and thin or flat and thick gingiva. (Cortellini & Bissada, 2018) According to a recent study that used previously reported parameters, "biotypes" can be classified into three categories. The first category is the thin scalloped biotype, which is associated with a slender triangular crown, subtle cervical convexity, interproximal contacts close to the incisal edge, a narrow zone of KT, clear thin delicate gingiva, and a relatively thin alveolar bone. The second category is the thick flat biotype, which is characterized by square-shaped tooth crowns, pronounced cervical convexity, large interproximal contact located more apically, a broad zone of KT, thick, fibrotic gingiva, and a comparatively thick alveolar bone. Finally, the third category is the thick scalloped biotype, which exhibits a thick fibrotic gingiva, slender teeth, narrow zone of KT, and a pronounced gingival scalloping (Caton et al., 2018; Zweers et al., 2014). The gingival phenotype has been linked to the long-term stability of periodontal health. Different methods to quantify the gingival phenotype have been described (Müller et al., 1999): (1) transgingival method (currently known as the gold standard), which comprises the insertion of an anesthetic needle until bone tissue or a tooth is reached presenting resistance to continued insertion; (2) Photography or visual examination where biotype is empirically classified as thin or thick; (3) Periodontal probing and the resulting transparency of the surrounding tissues that may allow for the visualization of the probe in thin phenotypes or may not when thicker phenotypes are present. (4) Real-time

ultrasonography has been a valuable diagnostic tool in the medical field for several decades. One of the most notable benefits of ultrasound is its ability to assess dynamic tissue perfusion noninvasively and instantaneously, indicating the degree of inflammation through color flow ultrasonography. This property has made it a popular choice in the medical field, including oral pathology. Ultrasound devices have been used to visualize and characterize the epithelium and connective tissue's thickness, echotexture, and pathological changes (Barootchi et al., 2022; Izzetti et al., 2021).

An intact interproximal papilla is a critical issue to clinicians, especially when it is between the maxillary central incisors (often termed the central papilla)(Tarnow et al., 1992). Due to its complex physiology, the central papilla either takes the shape of a pyramid or as a slight gingival col, depending on the location of the contact area and the height of the gingiva (Zetu & Wang, 2005). The presence, shape, size, and health of the central papilla affect the appearance of an individual (Chang, 2007) and hence the patient's satisfaction, so it is important to understand the factors that might affect the interproximal papilla integrity when placing an implant or when performing periodontal plastic surgery. Wheeler's Atlas of Tooth Form (Ash, 1984), described the level of the soft tissue in a single-implant supported restoration and the contralateral natural tooth, and found that the facio-lingual root diameter width and the proximal curvature of the cementoenamel junction can have a positive impact on the maintenance of the mesial papilla height at a single-implant supported restoration.

Soft tissues around implants have different considerations. It is widely believed that the ability of the mucosa to maintain the appropriate protection between the oral environment and implants can have a major impact on the long-term success of implants (Armitage et al.,

1977). Some authors reported that (Highfield, 2009; Souza et al., 2016) in patients with good oral hygiene, the marginal mucosa around implants was clinically healthy, and not affected with the absence of keratinized mucosa (KM). Other researchers reported an association between implant survival and width of KM (Kim et al., 2009; Salvi & Lang, 2004). In regards of mucogingival junction, researchers have reported tendency of MGJ to maintain its original position due to the muscular pull and genetic influence after its repositioning during surgery as described by Ainamo et. al ,1992 (Ainamo et al., 1992).

Statement of the Problem

Many of the aforementioned characteristics (color, texture, contour, consistency, papilla dimensions and height, stippling, and the width of keratinized mucosa) have been described for periodontal tissues of the natural tooth; however, few studies have described these characteristics of the peri-implant mucosa.

Objectives

The aims of this study were: 1) to compare these characteristics of the healthy gingiva around natural teeth with the appearance of mucosa around healthy implants, using clinical and photographic methods, including ultrasonography; and 2) to assess if tissue thickness correlates with the color of the gingiva of teeth and mucosa of implants.

Materials & Methods:

Study design & participants

33 patients with a total of 33 implants and 33 contralateral natural teeth were included in the study (20 males and 13 females, mean age = 66.5 years). Patients who met the inclusion and exclusion criteria were recruited through the Department of Periodontics and Oral Medicine at the University of Michigan, School of Dentistry and signed an informed consent to allow for participation in clinical examinations and the taking of pictures. The protocol was approved by the Institutional Review Board (IRB: HUM00194618) at the University of Michigan.

Minimum sample size was calculated using the paired χ^2 (Chi square) test in nQuery Advisor software with level of significance 0.5 and power of 80%. These preliminary calculations determined that a minimum of 19 implants and 19 healthy teeth were be needed for the study, which translates to (n=19) subjects. However, as this power calculation presents only the minimum required subject number, our team has determined that we will include 33 implants and 33 natural teeth from n=33 subjects, in order to collect sufficient baseline data to characterize the healthy peri-implant mucosa.

The characteristics of implants included in this study are listed in Supplemental Figure 6. In total, there were 18 bone level and 15 tissue level implants. Sample clinical photos of the patient population are included in Figure 22.

Inclusion & Exclusion criteria

Inclusion criteria were as follows: 18+ years of age; non-smoker; received at least one dental implant and has a corresponding contralateral natural tooth on the same arch; implant and tooth located in the anterior maxilla (premolar to premolar); healthy periodontal condition, as determined by absence of BOP (Zucchelli G, 2019). In this study, we arbitrarily defined periodontal health as a full-mouth BOP score of ≤ 30%.

Exclusion criteria were the following: Undergoing radiotherapy or having a history of radiotherapy; poor oral hygiene (BOP >30% on the examined arch); uncontrolled diabetes (HbA1c > 8); having known medical diseases and/or medications known to affect soft tissue characteristics (e.g., taking medication that may lead to gingival overgrowth; vesiculobullous diseases; lichen planus; hyperkeratosis associated with occlusal issues or traumatic oral hygiene habits; amalgam tattoo or adjacent amalgam restorations.

Null Hypotheses

The study was designed as a split-mouth cross-sectional design comparing hard and soft tissue characteristics of the healthy implant to the contralateral healthy natural tooth.

The null hypothesis had two parts:

1) The peri-implant buccal and interproximal tissues do not differ from the contralateral natural tooth of the same arch with regards to color, contour, form, consistency, texture, KTW, papilla dimensions, soft tissue thickness, or buccal bone thickness.

2) The thickness of the soft tissues is not associated with color changes compared with thin peri-implant phenotype.

Ultrasonography

An ultrasound imaging device (ZS3, Mindray, Mountain View, CA) with a custom-built prototype probe (measuring approx. 30 × 18 x 12 mm) was used to collect sagittal ultrasound slice data at the straight facial, mesial papilla, and distal papilla of the implant and the contralateral natural tooth. Measurements were conducted by a single operator (TH) in normal, perfusion, and power modes. Prior to data collection, the operator was calibrated against a gold standard experienced ultrasound operator (SB). Measurements of tthe buccal bone thickness, soft tissue thickness, and papilla heights were performed on normal mode images in Horos software version 3.3.6. Ultrasonographic "power" and "perfusion" modes were used, to determine the vascular perfusion of the buccal tissues. Power and perfusion were measured at the straight buccal, mesial papilla, and distal papilla of each implant and tooth.

Power and perfusion data of the buccal soft tissues was obtained via ultrasonography and analyzed in Pixel Flux (Version 1.0, Chameleon-Software, Leipzig, Germany). See Figures 1-5 for details.

Clinical measurements were collected by a single clinical examiner (TH). Prior to collecting clinical data, the examiner was calibrated against a gold-standard faculty (SS – not an author of the study). The intraclass correlation coefficient (ICC) used to assess the intra-examiner reliability of probing was 0.99 using a UNC-15 probe (Hu-

Friedy). KTW, papilla-contact distance, crown height, and papilla base distance were calibrated to an ICC of 0.96 using a 0.10-mm Boley gauge.

Camera and photography specifications

Digital photographs were taken using a Canon EOS 77D fitted with a 100mm macro lens and Canon MR14-EX II ring lite macro flash. Shutter speed was set to 1/80, Aperture (F) of 25, ISO 400, Exposure 0, Color mode: Faithful, color adjustment: Flash, Image quality: Large + RAW, and magnification 1:2. In order to ensure the most accurate color readings, it was necessary to eliminate glare from soft tissue reflections. For this reason, cross-polarized photography was conducted by attaching the Polar Eyes polarizing filter to the macro lens; to compensate for the reduced light flow through the lens, the ISO was adjusted to 1600 for all cross-polarized images. Color standardization of photos was performed using the ColorChecker Classic Nano color calibration card.

Camera RAW files were converted from CR2 to DNG (digital negative) format via the Adobe DNG Converter software (Supplemental Figure 1 and 2). Photos were then color standardized by processing the images with the ColorChecker Classic Nano card through the software “ColorChecker Camera Calibration.” (Supplemental Figure 3).

Color data was extracted from predefined zones of implants and teeth using 2x2 mm selections in Photoshop. Zones were defined as follows: The free gingival/mucosal margin zone was defined as a 2x2 mm Photoshop selection measured from the free margin. The attached gingiva / supracrestal tissue adhesion was measured as a 2x2 mm

selection from the sulcus depth and extending apically. The mucogingival junction zone was a 2x2 mm selection centered around the mucogingival junction. Lastly, the 2x2 mm mucosa zone was located apical to the mucogingival junction within the mucosal tissues. Image scale for the 2x2 mm selections was calibrated in Photoshop to the tenth of a millimeter using the crown heights obtained by clinical measurements with the Boley gauge (see "Clinical measurements: Calibration and measurement locations" section above). The scaled Photoshop images were then used to measure the papilla heights, the widths of papillas as measured between the zeniths of the adjacent teeth, and the space between the contact point and papilla tip, if present (Figure 5).

The rationale for using 2x2 mm selections stems from commercial intraoral spectrophotometers used in existing publications, which tend to analyze a 2x2 mm selection for color analysis (Czigola et al., 2021; Floriani et al., 2024; Liberato et al., 2019; Parameswaran et al., 2016; Witkowski et al., 2012). This study originally intended to use a commercial intraoral spectrophotometer, but due to the available USA companies going bankrupt during the 2019 pandemic, a study investigator (TH) had to devise this study's workaround method for determining color.

The acronym "CIELAB" abbreviates the French organization "Commission Internationale de l´Eclairage", or the Commission of Illumination (CIE, 2024). This organization created a standardized international format for measuring color values. CIELAB, also called CIE L*a*b*, classifies colors by their L*, a*, and b* values. The L* is a numerical value from 0 to 100 which describes the value of the color ("darkness or lightness"); 0 is pure black and 100 is pure white. The other values, a* and b*, describe the hue of a color. A* describes the hue along the red-green axis, where a negative a* value is green and positive a* is red; b* describes the yellow-blue axis, where a positive b* value is

yellow and a negative value is blue. The L*a*b* notation can be summarized in the following diagrams (Supplemental Figures 4 and 5).).

Statistical analyses

Descriptive data for all parameters were obtained, and the Data was analyzed in Excel and Rstudio in collaboration with a third-party data analyst. Statistical tests performed included paired T-square tests, correlation, multi-ANOVA, and linear regression analyses. Statistical significance was set at $p = .05$.

Results

The study sample comprised 33 implants and 33 contralateral natural teeth in 33 patients in a split-mouth study design. The demographic data of the patient population are shown in Table 1.

Papilla results

In our study, papilla heights were obtained via two separate methods: From photographs and from ultrasound. The Photoshop papilla measurements showed that implants had an average mesial papilla height of 3.0 ± 1.3 mm, whereas in teeth the mesial papilla height averaged 3.7 ± 1.0 mm (p = 0.00125). The distal papillas in implants averaged 2.2 ± 1.0 mm, and in teeth was 2.9 ± 1.3 mm (p = 0.0022). These results were statistically significant, but clinically differed by about 0.5mm. (Figure 21)

In contrast, the ultrasound data of papilla heights showed thatthatmesial vs. distal papillae for teeth and implants had NSSD in mesial and distal papilla heights (Table 4).). In implants, the average mesial papilla height was 2.7 ± 1.0 mm; in teeth it was 2.6 ± 0.7mm ($p = 0.72$). The distal papilla height in implants was 2.7 ± 0.9mm, and in teeth was 2.7 ± 0.8mm ($p = 0.74$). These ultrasound results showed no statistically significant differences in papilla heights when comparing implants to natural teeth.

These papilla height findings, and the discrepancy between the Photoshop photo measurements and the ultrasound measurements, are discussed further in the discussion section.

Additionally, the papilla widths were compared between implants and natural teeth. These results showed a statistically significant difference between the mesial papilla widths, but NSSD with regards to the distal papilla widths (Figure 21).

Furthermore, in our study we found that in teeth, the average horizontal (Bu-Li) tissue thickness at the papilla from the buccal bone is 1.3 ± 0.5mm. In implants, the average horizontal (Bu-Li) tissue thickness at the papilla from the buccal bone is 2.3 ± 0.7mm (Figure 23). This was found to be a statistically significant result and is discussed further in the discussion section.

Papillas were classified via the Nordland & Tarnow 1998 classification (Figure 4.) All 33 implants and 33 teeth in our study were Nordland Class I (having a papilla tip located between the interproximal CEJ and the contact point). A weak correlation was found between the distance from the bone crest to the papilla tip, and from the papilla tip to the contact point, as shown in Table 2.

Average implant and tooth measures are displayed in Figures 5 and 6.

Ultrasonographic buccal bone measurements

In our study, and as shown in Table 3, ultrasonography of the straight buccal of implants and teeth revealed buccal bone thickness did not appear to differ between implants vs. natural teeth, with a p-value of 0.18. Implant buccal bone averaged 0.7 mm ± 0.3, whereas tooth buccal bone averaged 0.63 mm ± 0.3.

However, our study determined there is a statistically significant difference regarding distance from the buccal bone crest (BBC) and the free gingival/mucosal margin (FG/MM). Implants had greater BBC-FMM distance compared to teeth. In implants, this distance was 4.13mm ± 1.5, whereas in natural teeth it was 2.9 mm ± 1.0. The p-value as determined via paired T-test was 1.9×10^{-4}.

Buccal soft tissue thickness

Implants in our study also demonstrated statistically thicker tissues than teeth (as seen in Table 4). Essentially, the buccal soft tissues of implants were statistically thicker at all predefined zones in this study and were on average ~0.8 mm thicker than the corresponding implant soft tissues (Figure 7).

The soft tissue thickness at the exact mucogingival junction area likewise revealed statistically thicker tissues at implant sites compared with tooth sites (Table 6). Implants had a mean thickness at the MGJ of 1.9mm ± 0.8, whereas in teeth, this was 1.2 ± 0.5mm, with a p-value of 5.31×10^{-5} as calculated by the paired T-test.

Probing depths, recession, BOP, and KTW

Statistically significant differences were found when comparing implant PDs to tooth PDs (Table 5). The average PDs for implants was 3.0 ± 0.7 mm, and in teeth was 2.5 ± 0.5 mm.

The majority of implants and teeth in our study exhibited no buccal recession and no BOP. Going by the Herrera et al. 2023 EFP workshop recommendations, implants were considered healthy if up to one (of its six) probing sites exhibited pinpoint BOP (Herrera et al., 2023).

Soft tissue thickness & underlying root or abutment visibility

One of the primary outcomes of our study involved analysis of the color of the soft tissues using CIELAB values.

In our study, analysis of the L* value (for the "darkness and lightness" of the tissues) allowed us to determine whether tissue thickness was correlated with implant abutment (or tooth root) visibility through the tissues. What we found was that soft tissue thickness showed a weak positive correlation with the L* value, indicating that thickness was indeed related to the shadow visibility of implant abutments. Likewise, the L* value showed a correlation with tissue thickness and the visibility of the tooth root (see Table 6).

In implants, a slight positive correlation of +0.16 between thickness and L* value suggests that thicker tissues result in lighter values of the supracrestal tissue adhesion of implants. Conversely, in natural teeth, the slight negative correlation of -0.07 suggests that thicker tissues result in darker color values of the supracrestal attachment zone.

Exploratory analyses (including ANOVA/ANCOVA analyses) were run to compare soft tissue thickness, ultrasonographic blood flow measurements, and the objective color measurements. No correlations were found.

CIELAB L*a*b* values: Color and its relationship to tissue thickness

Comparison of the individual CIELAB L*, a*, and b* values describing the lightness and hue of soft tissues between implants and teeth showed no statistically significant differences (Table 9). However, correlation and linear regression analyses suggest that soft tissue thickness is associated with changes in the hue and lightness of soft tissue, although the results were non-statistically significant.

The a* value in CIELAB notations describes the red-green color axis. Shifting towards a redder hue is indicated by a positive a* value. In contrast, shifting away from red and towards green is indicated by a negative a* value. In implants, for every 1mm increase in free gingival margin thickness, a* decreases by 3.69. This suggests that thicker tissues at the free gingival margin tend to be less red than thinner tissues. A similar finding occurs when examining the supracrestal tissue adhesion and its relationship to color. For every 1mm of attached mucosa thickness, a* decreases by 1.70 – again indicating a shift away from a red hue and more towards a greenish hue.

Intriguingly, teeth appeared to show an opposite relationship (Table 10). In teeth, for every 1mm increase in free gingival margin thickness, the a* increased by 2.09. For every 1mm increase in supracrestal tissue attachment thickness, a* increases by 0.03. This indicates that thicker tooth tissues appear redder than thinner tooth tissues.

The correlation charts comparing L*, a*, and b* values with soft tissue thickness for implants and teeth are shown as Figures 8 through 11.

The value of the tissues (amount of "lightness" or "darkness"), as described via the CIELAB L* value, likewise appeared to change with increasing soft tissue thickness (Figures 12-15). For every 1mm thickness increase at the free mucosal margin, Implants exhibited an L* increase of 2.38. Teeth showed a similar change; each 1mm thickness increase at the free gingival margin caused L* to increase by 2.10.

Similar functionality was noted at the supracrestal tissue adhesion of implants, where each 1mm thickness caused L* to go up by 2.38; in teeth, a slight decrease of 1.04 was noted.

Lastly, the CIELAB b* values describe hue changes along the blue-yellow color axis. In implants, each 1mm increase in free mucosa thickness resulted in a b* decrease of 1.87 – indicating a shift away from yellow and towards blue. In teeth, this relationship was positive, resulting in a 0.77 b* shift towards the yellow hue at the free gingival margin. (Figures 16-19).

Summary table: How color relates to soft tissue thickness?

The changes in CIELAB L*a*b* values with regards to tissue thicknesses are summarized in Table 11. Calculation of the p values using the paired T-test revealed that most of the findings did not show statistically significant differences, with the exception being the a* value at the implant free gingival margin (with a p value of 0.032).

ΔE comparing tooth vs. implant zones

As described in the Materials & Methods section, color measurement zones are defined as 2x2 mm areas measured at free gingival / mucosal margin, supracrestal tissue attachment / adhesion, at the MGJ, mucosa beyond MGJ, and mesial and distal papillas above the zenith-to-zenith line ("papilla base") (Figure 24).

Paired T-test analyses comparing ΔE between tooth vs. implant zones revealed no statistically significant findings (Table 14). Clinically, the ΔE color differences between tooth and implant zones are "barely perceptible" to "slightly perceptible" according to Sensient et al. 2024.

ΔE comparing implant zones to each other

We can see from Table 15 that the implant zones have a SSD in ΔE when comparing among zones. Specifically, color differences can be seen when comparing the free mucosal margin (FG) to supracrestal tissue adhesion (A); FG to mucosal (M); A to MGJ; A to M; MGJ to M; MGJ to the mesial papilla (MPAP); MGJ to the distal papilla (DPAP); M to MPAP; M to DPAP.

This can also be seen in the color visualization of average ΔE of zones for implants (Figure 25).

ΔE comparing tooth zones to each other

Similar to the implant results, we can see in Table 16 that when we compare the ΔE color differences between tooth zones, there is SSD in ΔE between the FG-MGJ, FG-M, FG-DPAP, A-MGJ, A-M, A-DPAP, MGJ-M, MGJ-MPAP, M-MPAP, M-DPAP, and MPAP-DPAP.

Color visualizations of the average ΔE of each zone for the teeth is shown in Figure 26.

Ultrasonographic Power and Perfusion: To compare vascularity of the tissues

Ultrasonographic power and perfusion analyses (used to quantify the amount of blood flow and flow velocity through the tissues) did not reveal statistically significant differences between implants and teeth. (Table 12). An example of the ultrasonographic images depicting power and perfusion is shown in Figure 20.

Qualitative measurements: Texture, form, consistency

The texture, form, and consistency of the tissues were qualitatively evaluated. With regards to texture, both implants and natural teeth exhibited stippling. 27 of 33 teeth, and 27 of 33 implants, had stippling; and stippling was bilaterally mirrored in patients regardless of whether the site was an implant or a natural tooth. With regards to consistency: Both implants and natural teeth exhibited resilient soft tissues that rebound after pressure was clinically applied. With regards to form, all sites exhibited scalloping of the gingival margins regardless of whether it was an implant or a tooth site.

ANOVA and ANCOVA analyses

Exploratory analyses (including ANOVA/ANCOVA analyses) were run to compare soft tissue thickness, ultrasonographic blood flow measurements, and the objective color measurements. **Implant bucco-lingual position**

Implant bucco-lingual position was qualitatively determined based upon the location of the screw channel. It was found that of the 33 total implant crowns, 17 were cement-retained

and 16 were screw-retained. All screw-retained implant crowns had emergence from the cingulum (for incisors / canines) or from the central groove (for premolars). It was not possible to exactly determine the implant position without removing the crown, due to the likelihood of the restorative dentists using custom angulated abutments. Likewise, this study did not include CBCT's, and therefore, exact implant bucco-lingual position could not be determined.

(See Supplemental Figure 7 for analysis result).

Discussion

The objective of this study was to conduct a split-mouth clinical study to characterize the healthy peri-implant mucosa, using the contralateral natural teeth as comparison.

Our study confirms existing evidence that implants have a trend towards thicker buccal soft tissues than teeth (about 0.8mm thicker) – due in part to the concave emergence profile allowing a thicker tissue fill on the facial aspect of the implant prosthesis (Abu Hussien et al., 2023; Barootchi et al., 2022; Barootchi et al., 2020; Jun et al., 2013; Müller et al., 1999; Thoma et al., 2014; Zucchelli et al., 2020). Implants demonstrate thicker tissues in this area because the concave profile of implant abutments create greater soft tissue fill, compared to the straight tooth root (Figure 7).

Our findings on buccal implant tissue thickness support previous literature on the topic. Hussein et al. in 2023 performed a cross-sectional study examining palatal tissue thickness of healthy teeth and implants, and found that implants consistently had thicker palatal mucosa than the contralateral teeth, measuring 4.58 ± 1.38 mm at the pocket base

(compared to the 3.01 ± 1.11 in teeth), and 3.58mm ± 2.15 at 3mm coronally from the base of the pocket, compared with 1.89 ± 1.11 in the contralateral teeth (Abu Hussien et al., 2023). Likewise, the 2017 World Workshop article on peri-implant health by Araujo and colleagues describe how the healthy peri-implant mucosa patients with a "flat-thick" phenotype tended to have greater dimensions of the peri-implant mucosa, compared with their natural teeth. This effect was less pronounced in patients with a thin-scalloped phenotype.

Our study also supports the idea that implant-retained prostheses have the ability to reduce the distance from papilla tip to contact point via prosthetic shaping (Chow & Wang, 2010; Flanagan, 2015; Gobbato et al., 2013; Jamilian et al., 2015; Urban et al., 2021). In our study, implant papillae had a nearly 50% less prevalence of papilla deficiency compared with natural teeth. When a space was present, implants had less distance, measuring 0.1 mm on average and ranging from 0 - 1.4 mm; teeth correspondingly had greater space, measuring 0.4 mm and ranging from 0 to 2.4 mm. Papillaheight is important for esthetics. A lack of papilla height can appear as a small "black triangle" between the teeth, which may be visible when the patient smiles (Singh et al., 2013).

AA valid critique of this study with regards to papilla measurements is that the inclusion/exclusion criteria did not explicitly exclude teeth with crowns, subgingival restorations, or recessions. Therefore, it is possible that the restorations of the teeth affected the papilla heights as well.

Another point of contention in this study was the potential for distortion in the Photoshop-based photo measurements. The photos may have some foreshortening / curvature errors (due to the arch curving distally from anterior to posterior), even despite attempting to standardize the photos to be "straight-on" shots. This study included many 2nd premolars in

the patient population, and despite using special posterior black retractors, it was difficult to fully stretch the cheek of these patients (many of whom were overweight) to fully show the distal papillas of the 2nd premolars in a straight-on-shot. Therefore, although the data analysis from Photoshop measurements indicated a statistically significant difference between the mesial and distal papillas between implants and teeth, these results should be interpreted with caution due to potential errors introduced via measurement distortion caused by photo perspective.

In contrast to the Photoshop-based papilla measurements, the ultrasound papilla height measurements posed less risk of distortion due to the fact that each papilla was directly measured with the ultrasound sensor. Therefore, the ultrasound papilla heights were ostensibly more accurate than the Photoshop photo-based measurements. Because the ultrasound papilla height measurements showed no statistically significant differences between implant vs. tooth papilla heights, we can conclude within the limitations of this study that there is no difference in papilla heights when comparing implatns to natural teeth.

Furthermore - all patients in this study were recruited from the periodontics department's "perio maintenance" patient pool -- and therefore, the majority of these patients had recession present (although they were periodontally healthy). This perio maintenance patient pool may be predisposed to have significantly shorter papillas than the "normal range" due to interproximal recession, compared to a healthy young "normal" population without history of periodontal disease. Likewise, the implant patient pool tends to be older rather than younger, and age contributes to recession as described by Billings et al 2018. The average papilla height of 2.7 as found in our study from ultrasound measurements does correlate with the biologic widths described by Vacek et al. 1994 and Gargiulo et al 1961, wherein the

human body creates an average tissue height of about 1.0 mm for the sulcus, plus about 2 mm tissue height for the connective tissue and epithelium.

Our study also found that implants tend to have greater distance from the facial buccal bone to the free mucosal margin. In implants, this distance was 4.13 mm ± 1.5, whereas in natural teeth it was 2.9 mm ± 1.0. The p-value as determined via paired T-test was 1.9×10^{-4}.

Our study also found that papilla thickness is slightly greater in implants as compared to natural teeth. In teeth the average horizontal (Bu-Li) tissue thickness at the papilla from the buccal bone is 1.3 ± 0.5mm, and in implants this was 2.3 ± 0.7mm (Figure 23). This may be due to the fact that the emergence profile of the implant crown creates a greater soft tissue thickness not only at the straight buccal aspect, but also interproximally at the papillas, when compared to natural teeth.

Buccal bone is an important component of peri-implant and periodontal health (Berglundh et al., 2018; Monje et al., 2019; Monje et al., 2023). One of the key concerns with implants is that buccal bone of an edentulate site undergoes remodeling over time (Cicciù et al., 2023; Pagni et al., 2012; Spray et al., 2000; Temmerman et al., 2015). A noninvasive way to determine buccal bone thickness and position is to perform ultrasonographic analysis.

Therefore, this BBC-FMM finding indicates that healthy implants naturally have a thicker supracrestal tissue adhesion compared to the contralateral tooth's supracrestal tissue attachment (Araujo & Lindhe, 2018). One possible reason for this may be remodeling. After tooth extraction, the buccal bone undergoes remodeling (Amler, 1981; Spray et al., 2000). Furthermore, many clinicians place implant platforms subcrestally, which may likewise

encourage remodeling of the peri-implant hard tissues. Where hard tissue resorbs, soft tissue tends to fill. Implants are also known to have deeper pocket depths that are considered healthy compared to natural teeth (Souza et al., 2016).

Implants also demonstrated statistically thicker buccal tissues and deeper probing depths than teeth. Implant buccal tissues were on average ~0.8 mm thicker than the corresponding implant soft tissues. Probing depths measured 3.0 ±0.7 mm in implants, and 2.5 ± 0.5 mm in teeth. Our findings support previous literature citing that healthy implants have deeper PD's compared with teeth (Christensen et al., 1997; Coli & Sennerby, 2019; Herrera et al., 2023; Parpaiola et al., 2015; Pathak et al., 2016; Schou et al., 2002). This phenomenon is due to the fact that teeth have supracrestal tissue attachment via Sharpey's fibers inserting into cementum, whereas implants lack such fibers and therefore are less resistant to probing forces (Etter et al., 2002).

One of the predominant findings of our study is that soft tissue thickness appears correlated with color, though more studies of larger sample size are required to rigorously test the finding. Our study developed a method of determining standardized color measurements without an intraoral spectrophotometer. Our color analyses demonstrate that buccal tissue thickness has a weak inverse relationship with the L* value, indicating that increased thickness is correlated with reduced shadow visibility of implant abutments and tooth roots (Table 8). However, the overall color (combined L*a*b* values) of implant vs. tooth tissues were statistically insignificant (Table 10).

So when does a color difference become clinically relevant? It becomes relevant if, for example, a periodontal surgical procedure results in a gingival color change that is

perceivable to the average human eye. This perceivable color difference is characterized by "ΔE" (read as "delta E"). Delta E is described in Table 7.

Delta E is calculated by the formula:

$$\Delta E = SqRt((L_2\text{-}L_2L_1)^2 \text{–+} (a_2\text{-}a_1)^2 \text{–+} (b_2\text{-}b_1)^2)$$

, which considers all three of the L*, a*, and b* values described earlier.

Our data indicates that there are no statistically significant differences in the combined L*a*b* values when comparing implants vs. natural teeth (Table 8).

In situations of esthetic soft tissue grafting, soft tissue color differences become very clinically relevant. Most clinicians avoid free gingival grafting in the esthetic zone due to the marked color discrepancies between the grafted and nongrafted sites (Cairo, 2017; Emilov & Deliverska-Aleksandrova, 2022; Jenabian et al., 2016; Raoofi et al., 2019; Thoma et al., 2014; Zucchelli et al., 2020). Witzel et al. 1973 noted that although individuals perceive color differently, but most humans are able to discern differences of lightness, hue, and saturation with a certain degree of precision (Witzel et al., 1973). The most reliable way to quantify color differences is by using quantitative color analysis.

Our findings confirm that root prominence in thin periodontal tissues results in the light-colored root being visible through the tissues, and that thin periodontal tissues around implant abutments results in the implant abutment being visible, due to the abutment's darker metallic color.

Implant bucco-lingual position was examined based on determining the position of the implant crown screw channel. It was found that of the 33 total implant crowns, 17 were

cement-retained. This means only 16 of the were screw-retained. All screw-retained implant crowns had emergence from the cingulum (for incisors / canines) and from the central groove (for premolars). It was not possible to exactly determine the implant position without removing the crown, due to the presence of custom angulated abutments. Likewise, this study did not obtain CBCT's, and therefore, exact implant bucco-lingual position could not be determined. However, we can speculate that implant bucco-lingual position may influence tissue thickness or color, especially in cases with a thin periodontal phenotype and loss of buccal bone. In these situations, the implant abutment and/or implant body may appear as a dark shadow seen through the thin gingiva. A literature search in PubMed indicates that few existing studies examine this phenomenon, and may be an area for future investigation in the field.

Implant position may be a factor influencing tissue color. Although our study was unable to determine correlations between implant position and color due to lack of CBCT and lack of approval to remove implant crowns, there are existing studies on this topic. For example, it is known that the soft tissue profile and subsequently, the emergence profile of the implant restoration, is influenced by the 3D spatial position of the implant during placement (Chu et al., 2019). Likewise, implant placement may lead to the resorption of buccal bone and subsequent apical migration of the mucosal margin (Chen & Buser, 2014). However, whereas bone readily remodels following an extraction or other surgical trauma, soft tissue phenotype (the “tissue thickness”) tends to stay consistent unless it is modified via soft tissue augmentation, as soft tissue thickness is predominantly determined by an individual’s genetics (Amler, 1981; Gargiulo et al., 1961; Temmerman et al., 2015).

No statistically significant differences were observed with regards to buccal bone thickness, KTW, BOP, recession, papilla heights, and vascular flow as measured by ultrasonographic power and perfusion analyses. Likewise, no statistical differences were found regarding the qualitative measures of stippling, gingival margin contour, form, consistency. ANOVA and ANCOVA analyses were inconclusive, per Supplemental Figure 7.

Therefore, we can conclude that the null hypotheses of the study were partially rejected.

In conclusion, our data suggests the healthy peri-implant mucosa can be characterized as Table 13.

Study Limitations

This study notably has several limitations. Should future studies aim to expand upon this research, it would be wise to address the following limitations:

- Case selection: Our study did not explicitly exclude certain factors which may have influenced the results, such as: adjacent teeth with subgingival crown or composite margins; adjacent implants or bridges; tissue-level implants.
- Ultrasound: One major limitation of ultrasound is its inability to detect buccal bone thickness beyond 1mm. This may have influenced the final buccal bone average thicknesses, because the maximum possible measurable buccal bone thickness was 1mm.
- Operator dependency: Ultrasound is an operator-dependent clinical measurement modality, and the image accuracy may be influenced by factors such as bubbles

within the ultrasonography gel, thickness of the prepared gel pad against the sensor, amount of pressure applied during measurements, and the angulation of the probe.

- Limited sample size: The study is composed of 66 total implants and natural teeth, in a split-mouth design. Post-hoc analyses of sample size in G-power suggests that the study was somewhat underpowered, which may explain several of the non-statistically significant results found in the study. Future studies should aim to have 300 total implants and natural teeth for sufficient power.
- Color quantification: The color analysis procedure utilized in this study had multiple steps. A commercial intraoral spectrophotometer might reduce error due to the fewer number of steps in the color analysis workflow.
- Lack of longitudinal or interventional data: To further investigate the influence of tissue thickness on tissue color, rather than conducting a split-mouth study (comparing contralateral teeth to implants), it may be more advantageous from a standardization standpoint to perform analyses on single tooth sites undergoing soft tissue grafting. This would eliminate potential confounding variables and differences found between contralateral teeth and implants.
- Statistical shortcomings: Multi-ANOVA analysis was attempted, but the F-value was high, indicating heterogeneity among variables. Therefore, Multi-ANOVA was inconclusive.

To conclude, our study shows some promising data trends, but the data should be interpreted with caution due to the aforementioned limitations. Future studies may address these limitations to provide more illuminating data.

Future implications

The development of the color analysis workflow of this study may be useful for other clinical applications, such as: Determining color shade matches for esthetic restorations; and to determine "color maps" for teeth to allow technicians to produce very natural-looking crowns for anterior esthetic areas. The methods of this study could also be used in future soft- or hard-tissue grafting cases, to track the changes in tisue thickness and color over time.

AUTHOR CONTRIBUTIONS

Teresa Heck: Investigation (lead); writing—original draft (lead); data collection and analysis (lead); writing—review and editing (lead). **Hom-Lay Wang**: Project administration (lead); validation (lead). **Asfandyar Tariq Sheikh**: Investigation (supporting); data collection (supporting); writing – review and editing (supporting). **Khushboo Kalani:** Investigation (supporting); data collection (supporting); writing – review and editing (supporting). **Shayan Barootchi**: Writing – review and editing (supporting). **I-Ching Wang**: Writing – review and editing (supporting). **Junying Li**: Writing – review and editing (supporting).

FUNDING INFORMATION

Study supported in part by the Rackham Graduate Student Research Grant of the University of Michigan, and the Delta Dental Fund Grant, Award Number: AWD021537.

CONFLIC T OF INTEREST STATEMENT

The authors declare no conflicts of interest.

References

Abrahamsson, I., Berglundh, T., Glantz, P. O., & Lindhe, J. (1998). The mucosal attachment at different abutments. An experimental study in dogs. *J Clin Periodontol*, *25*(9), 721-727. https://doi.org/10.1111/j.1600-051x.1998.tb02513.x

Abu Hussien, H., Machtei, E. E., Khutaba, A., Gabay, E., & Zigdon Giladi, H. (2023). Palatal soft tissue thickness around dental implants and natural teeth in health and disease: A cross sectional study. *Clin Implant Dent Relat Res*, *25*(2), 215-223. https://doi.org/10.1111/cid.13171

Afshar-Mohajer, K., & Stahl, S. S. (1977). The remodeling of human gingival tissues following gingivectomy. *J Periodontol*, *48*(3), 136-139. https://doi.org/10.1902/jop.1977.48.3.136

Ainamo, A., Bergenholtz, A., Hugoson, A., & Ainamo, J. (1992). Location of the mucogingival junction 18 years after apically repositioned flap surgery. *J Clin Periodontol*, *19*(1), 49-52. https://doi.org/10.1111/j.1600-051x.1992.tb01148.x

Albrektsson, T., Zarb, G., Worthington, P., & Eriksson, A. R. (1986). The long-term efficacy of currently used dental implants: a review and proposed criteria of success. *Int J Oral Maxillofac Implants*, *1*(1), 11-25.

Amler, M. H. (1981). The lag phase factor in bone healing. *Journal of Periodontal Research*, *16*(6), 617-627. https://doi.org/https://doi.org/10.1111/j.1600-0765.1981.tb01000.x

Araujo, M. G., & Lindhe, J. (2018). Peri-implant health. *J Clin Periodontol*, *45 Suppl 20*, S230-s236. https://doi.org/10.1111/jcpe.12952

Armitage, G. C., Svanberg, G. K., & Löe, H. (1977). Microscopic evaluation of clinical measurements of connective tissue attachment levels. *J Clin Periodontol*, *4*(3), 173-190. https://doi.org/10.1111/j.1600-051x.1977.tb02271.x

Ash, M. M. (1984). *Wheeler's atlas of tooth form* (5th ed.). W.B. Saunders Company.

Barootchi, S., Tavelli, L., Di Gianfilippo, R., Shedden, K., Oh, T.-J., Rasperini, G., Neiva, R., Giannobile, W. V., & Wang, H.-L. (2022). Soft tissue phenotype modification predicts gingival margin long-term (10-year) stability: Longitudinal analysis of six randomized clinical trials. *Journal of Clinical Periodontology*, *49*(7), 672-683. https://doi.org/https://doi.org/10.1111/jcpe.13641

Barootchi, S., Tavelli, L., Zucchelli, G., Giannobile, W. V., & Wang, H. L. (2020). Gingival phenotype modification therapies on natural teeth: A network meta-analysis. *J Periodontol*, *91*(11), 1386-1399. https://doi.org/10.1002/jper.19-0715

Benic, G. I., Wolleb, K., Sancho-Puchades, M., & Hämmerle, C. H. (2012). Systematic review of parameters and methods for the professional assessment of aesthetics in dental implant research. *J Clin Periodontol*, *39 Suppl 12*, 160-192. https://doi.org/10.1111/j.1600-051X.2011.01840.x

Berglundh, T., Armitage, G., Araujo, M. G., Avila-Ortiz, G., Blanco, J., Camargo, P. M., Chen, S., Cochran, D., Derks, J., Figuero, E., Hämmerle, C. H. F., Heitz-Mayfield, L. J. A., Huynh-Ba, G., Iacono, V., Koo, K. T., Lambert, F., McCauley, L., Quirynen, M., Renvert, S., . . . Zitzmann, N. (2018). Peri-implant diseases and conditions: Consensus report of workgroup 4 of the 2017 World Workshop on the Classification of Periodontal and Peri-Implant Diseases and Conditions. *J Clin Periodontol*, *45 Suppl 20*, S286-s291. https://doi.org/10.1111/jcpe.12957

Cairo, F. (2017). Periodontal plastic surgery of gingival recessions at single and multiple teeth. *Periodontol 2000*, *75*(1), 296-316. https://doi.org/10.1111/prd.12186

Caton, J. G., Armitage, G., Berglundh, T., Chapple, I. L. C., Jepsen, S., Kornman, K. S., Mealey, B. L., Papapanou, P. N., Sanz, M., & Tonetti, M. S. (2018). A new classification scheme for periodontal and peri-implant diseases and conditions - Introduction and key changes from the 1999 classification. *J Clin Periodontol*, *45 Suppl 20*, S1-s8. https://doi.org/10.1111/jcpe.12935

Chang, L. C. (2007). The association between embrasure morphology and central papilla recession. *J Clin Periodontol*, *34*(5), 432-436. https://doi.org/10.1111/j.1600-051X.2007.01072.x

Chen, S. T., & Buser, D. (2014). Esthetic outcomes following immediate and early implant placement in the anterior maxilla--a systematic review. *Int J Oral Maxillofac Implants*, *29 Suppl*, 186-215. https://doi.org/10.11607/jomi.2014suppl.g3.3

Chow, Y. C., & Wang, H. L. (2010). Factors and techniques influencing peri-implant papillae. *Implant Dent*, *19*(3), 208-219. https://doi.org/10.1097/ID.0b013e3181d43bd6

Christensen, M. M., Joss, A., & Lang, N. P. (1997). Reproducibility of automated periodontal probing around teeth and osseointegrated oral implants. *Clin Oral Implants Res*, *8*(6), 455-464. https://doi.org/10.1034/j.1600-0501.1997.080603.x

Chu, S. J., Kan, J. Y., Lee, E. A., Lin, G. H., Jahangiri, L., Nevins, M., & Wang, H. L. (2019). Restorative Emergence Profile for Single-Tooth Implants in Healthy Periodontal Patients: Clinical Guidelines and Decision-Making Strategies. *Int J Periodontics Restorative Dent*, *40*(1), 19-29. https://doi.org/10.11607/prd.3697

Cicciù, M., Pratella, U., Fiorillo, L., Bernardello, F., Perillo, F., Rapani, A., Stacchi, C., & Lombardi, T. (2023). Influence of buccal and palatal bone thickness on post-surgical marginal bone changes around implants placed in posterior maxilla: a multi-centre prospective study. *BMC Oral Health*, *23*(1), 309. https://doi.org/10.1186/s12903-023-02991-3

CIE. (2024). CIE's objectives [web article]. https://cie.co.at/about-cie-0/cie-s-objectives

Coli, P., & Sennerby, L. (2019). Is Peri-Implant Probing Causing Over-Diagnosis and Over-Treatment of Dental Implants? *J Clin Med*, *8*(8). https://doi.org/10.3390/jcm8081123

Cortellini, P., & Bissada, N. F. (2018). Mucogingival conditions in the natural dentition: Narrative review, case definitions, and diagnostic considerations. *J Periodontol*, *89 Suppl 1*, S204-s213. https://doi.org/10.1002/jper.16-0671

Czigola, A., Róth, I., Vitai, V., Fehér, D., Hermann, P., & Borbély, J. (2021). Comparing the effectiveness of shade measurement by intraoral scanner, digital spectrophotometer, and visual shade assessment. *J Esthet Restor Dent*, *33*(8), 1166-1174. https://doi.org/10.1111/jerd.12810

Datacolor. (2024). The science of how we see color - and why we need spectrophotometers. https://www.datacolor.com/business-solutions/blog/why-we-cant-agree-color-perception/

Emilov, D. K., & Deliverska-Aleksandrova, E. G. (2022). Treatment of gingival recession with hypersensitivity using free soft-tissue graft procedures. *Folia Med (Plovdiv)*, *64*(2), 321-326. https://doi.org/10.3897/folmed.64.e62532

Etter, T. H., Håkanson, I., Lang, N. P., Trejo, P. M., & Caffesse, R. G. (2002). Healing after standardized clinical probing of the perlimplant soft tissue seal: a histomorphometric study in dogs. *Clin Oral Implants Res*, *13*(6), 571-580. https://doi.org/10.1034/j.1600-0501.2002.130601.x

Ferrari, M., Carrabba, M., Vichi, A., Goracci, C., & Cagidiaco, M. C. (2017). Influence of Abutment Color and Mucosal Thickness on Soft Tissue Color. *Int J Oral Maxillofac Implants*, *32*(2), 393–399. https://doi.org/10.11607/jomi.4794

Flanagan, D. (2015). Gingival Embrasure Fill In Fixed Implant-Supported Prosthetics: A Review. *J Oral Implantol*, *41*(6), e297-300. https://doi.org/10.1563/aaid-joi-D-14-00185

Floriani, F., Jurado, C. A., Abuhammoud, S., Vargas, M., Fischer, N. G., Rojas-Rueda, S., & Lopes, G. C. (2024). A Comparative Study of Shade-Matching Reproducibility Using an Intraoral Scanner and a Spectrophotometer. *Dent J (Basel)*, *12*(3). https://doi.org/10.3390/dj12030062

Gargiulo, A. W., Wentz, F. M., & Orban, B. J. (1961). Dimensions and Relations of the Dentogingival Junction in Humans. *Journal of Periodontology*, *32*, 261-267.

Gobbato, L., Paniz, G., Mazzocco, F., Chierico, A., Tsukiyama, T., Levi, P. A., Jr., & Weisgold, A. S. (2013). Significance of crown shape in the replacement of a central incisor with a single implant-supported crown. *Quintessence Int*, *44*(5), 407-413. https://doi.org/10.3290/j.qi.a29146

Haffajee, A. D., Socransky, S. S., & Goodson, J. M. (1992). Subgingival temperature (I). Relation to baseline clinical parameters. *J Clin Periodontol*, *19*(6), 401-408. https://doi.org/10.1111/j.1600-051x.1992.tb00670.x

Herrera, D., Berglundh, T., Schwarz, F., Chapple, I., Jepsen, S., Sculean, A., Kebschull, M., Papapanou, P. N., Tonetti, M. S., Sanz, M., participants, t. E. w., & consultant, m. (2023). Prevention and treatment of peri-implant diseases—The EFP S3 level clinical practice guideline. *Journal of Clinical Periodontology*, *50*(S26), 4-76. https://doi.org/https://doi.org/10.1111/jcpe.13823

Highfield, J. (2009). Diagnosis and classification of periodontal disease. *Aust Dent J*, *54 Suppl 1*, S11-26. https://doi.org/10.1111/j.1834-7819.2009.01140.x

Hunter, R. S. (1987). The measurement of appearance. In R. W. Harold (Ed.), (2nd ed. ed.). New York :: Wiley.

Izzetti, R., Vitali, S., Aringhieri, G., Nisi, M., Oranges, T., Dini, V., Ferro, F., Baldini, C., Romanelli, M., Caramella, D., & Gabriele, M. (2021). Ultra-High Frequency Ultrasound, A Promising Diagnostic Technique: Review of the Literature and Single-Center Experience. *Can Assoc Radiol J*, *72*(3), 418-431. https://doi.org/10.1177/0846537120940684

Jamilian, A., Perillo, L., & Rosa, M. (2015). Missing upper incisors: a retrospective study of orthodontic space closure versus implant. *Prog Orthod*, *16*, 2. https://doi.org/10.1186/s40510-015-0072-2

Jenabian, N., Bahabadi, M. Y., Bijani, A., & Rad, M. R. (2016). Gingival Unit Graft Versus Free Gingival Graft for Treatment of Gingival Recession: A Randomized Controlled Clinical Trial. *J Dent (Tehran)*, *13*(3), 184-192.

Jepsen, S., Caton, J. G., Albandar, J. M., Bissada, N. F., Bouchard, P., Cortellini, P., Demirel, K., de Sanctis, M., Ercoli, C., Fan, J., Geurs, N. C., Hughes, F. J., Jin, L., Kantarci, A., Lalla, E., Madianos, P. N., Matthews, D., McGuire, M. K., Mills, M. P., . . . Yamazaki, K. (2018). Periodontal manifestations of systemic diseases and developmental and acquired conditions: Consensus report of workgroup 3 of the 2017 World Workshop on the Classification of Periodontal and Peri-Implant Diseases and Conditions. *Journal of Periodontology*, *89*(S1), S237-S248. https://doi.org/https://doi.org/10.1002/JPER.17-0733

Jun, S. H., Ahn, J. S., Chang, B. M., Lee, J. D., Ryu, J. J., & Kwon, J. J. (2013). In vivo measurements of human gingival translucency parameters. *Int J Periodontics Restorative Dent*, *33*(4), 427-434. https://doi.org/10.11607/prd.1497

Jung, R. E., Holderegger, C., Sailer, I., Khraisat, A., Suter, A., & Hämmerle, C. H. (2008). The effect of all-ceramic and porcelain-fused-to-metal restorations on marginal peri-implant soft tissue color: a randomized controlled clinical trial. *Int J Periodontics Restorative Dent*, *28*(4), 357-365.

Kim, B. S., Kim, Y. K., Yun, P. Y., Yi, Y. J., Lee, H. J., Kim, S. G., & Son, J. S. (2009). Evaluation of peri-implant tissue response according to the presence of keratinized mucosa. *Oral Surg Oral Med Oral Pathol Oral Radiol Endod*, *107*(3), e24-28. https://doi.org/10.1016/j.tripleo.2008.12.010

Kleinheinz, J., Büchter, A., Fillies, T., & Joos, U. (2005). Vascular basis of mucosal color. *Head Face Med*, *1*, 4. https://doi.org/10.1186/1746-160x-1-4

Liberato, W. F., Barreto, I. C., Costa, P. P., de Almeida, C. C., Pimentel, W., & Tiossi, R. (2019). A comparison between visual, intraoral scanner, and spectrophotometer shade matching: A clinical study. *J Prosthet Dent*, *121*(2), 271-275. https://doi.org/10.1016/j.prosdent.2018.05.004

Löe, H., & Wright, W. H. (1965). Gingivectomy. *Odontol Tidskr*, *73*(5), 501-514.

Michalakis, K. X., Hirayama, H., Sfolkos, J., & Sfolkos, K. (2004). Light transmission of posts and cores used for the anterior esthetic region. *Int J Periodontics Restorative Dent*, *24*(5), 462-469. https://doi.org/10.11607/prd.00.0599

Monje, A., Chappuis, V., Monje, F., Muñoz, F., Wang, H.-L., Urban, I., & Buser, D. (2019). The Critical Peri-implant Buccal Bone Wall Thickness Revisited: An Experimental Study in the Beagle Dog. *The International journal of oral & maxillofacial implants*, *34*. https://doi.org/10.11607/jomi.7657

Monje, A., Roccuzzo, A., Buser, D., & Wang, H. L. (2023). Influence of buccal bone wall thickness on the peri-implant hard and soft tissue dimensional changes: A systematic review. *Clin Oral Implants Res*, *34*(3), 157-176. https://doi.org/10.1111/clr.14029

Mühlemann, H. R., & Son, S. (1971). Gingival sulcus bleeding--a leading symptom in initial gingivitis. *Helv Odontol Acta*, *15*(2), 107-113.

Müller, H. P., Schaller, N., & Eger, T. (1999). Ultrasonic determination of thickness of masticatory mucosa: a methodologic study. *Oral Surg Oral Med Oral Pathol Oral Radiol Endod*, *88*(2), 248-253. https://doi.org/10.1016/s1079-2104(99)70123-x

Ochsenbein, C., & Ross, S. (1969). A reevaluation of osseous surgery. *Dent Clin North Am*, *13*(1), 87-102.

Pagni, G., Pellegrini, G., Giannobile, W. V., & Rasperini, G. (2012). Postextraction alveolar ridge preservation: biological basis and treatments. *Int J Dent*, *2012*, 151030. https://doi.org/10.1155/2012/151030

Parameswaran, V., Anilkumar, S., Lylajam, S., Rajesh, C., & Narayan, V. (2016). Comparison of accuracies of an intraoral spectrophotometer and conventional visual method for shade matching using two shade guide systems. *J Indian Prosthodont Soc*, *16*(4), 352-358. https://doi.org/10.4103/0972-4052.176537

Parpaiola, A., Cecchinato, D., Toia, M., Bressan, E., Speroni, S., & Lindhe, J. (2015). Dimensions of the healthy gingiva and peri-implant mucosa. *Clin Oral Implants Res*, *26*(6), 657-662. https://doi.org/10.1111/clr.12359

Pathak, A. K., Goel, K., Shakya, V., & Tiwari, A. K. (2016). Periodontal parameters around implants and natural teeth. *Natl J Maxillofac Surg*, *7*(1), 52-55. https://doi.org/10.4103/0975-5950.196130

Raoofi, S., Asadinejad, S. M., & Khorshidi, H. (2019). Evaluation of Color and Width of Attached Gingiva Gain in Two Surgical Techniques: Free Gingival Graft and Connective Tissue Graft Covered By Thin Mucosal Flap, a Clinical Trial. *J Dent (Shiraz)*, *20*(4), 224-231. https://doi.org/10.30476/dentjods.2019.44916

Salvi, G. E., & Lang, N. P. (2004). Diagnostic parameters for monitoring peri-implant conditions. *Int J Oral Maxillofac Implants*, *19 Suppl*, 116-127.

Schou, S., Holmstrup, P., Stoltze, K., Hjørting-Hansen, E., Fiehn, N. E., & Skovgaard, L. T. (2002). Probing around implants and teeth with healthy or inflamed peri-implant mucosa/gingiva. A histologic comparison in cynomolgus monkeys (Macaca fascicularis). *Clin Oral Implants Res*, *13*(2), 113-126. https://doi.org/10.1034/j.1600-0501.2002.130201.x

Sensient. (2024). How do we calculate a perceptible color difference? https://www.sensientindustrial.com/na/color-college/how-to-choose-color/how-do-we-calculate-a-perceptible-difference

Singh, V. P., Uppoor, A. S., Nayak, D. G., & Shah, D. (2013). Black triangle dilemma and its management in esthetic dentistry. *Dent Res J (Isfahan)*, *10*(3), 296-301.

Souza, A. B., Tormena, M., Matarazzo, F., & Araújo, M. G. (2016). The influence of peri-implant keratinized mucosa on brushing discomfort and peri-implant tissue health. *Clin Oral Implants Res*, *27*(6), 650-655. https://doi.org/10.1111/clr.12703

Spray, J. R., Black, C. G., Morris, H. F., & Ochi, S. (2000). The influence of bone thickness on facial marginal bone response: stage 1 placement through stage 2 uncovering. *Ann Periodontol*, *5*(1), 119-128. https://doi.org/10.1902/annals.2000.5.1.119

Tarnow, D. P., Magner, A. W., & Fletcher, P. (1992). The effect of the distance from the contact point to the crest of bone on the presence or absence of the interproximal dental papilla. *J Periodontol*, *63*(12), 995-996. https://doi.org/10.1902/jop.1992.63.12.995

Tatakis, D. N., & Trombelli, L. (2004). Modulation of clinical expression of plaque-induced gingivitis. I. Background review and rationale. *J Clin Periodontol*, *31*(4), 229-238. https://doi.org/10.1111/j.1600-051x.2004.00477.x

Temmerman, A., Keestra, J., Coucke, W., Teughels, W., & Quirynen, M. (2015). The outcome of oral implants placed in bone with limited bucco-oral dimensions: A 3-year follow-up study. *Journal of Clinical Periodontology*, *42*. https://doi.org/10.1111/jcpe.12376

Thoma, D. S., Buranawat, B., Hämmerle, C. H., Held, U., & Jung, R. E. (2014). Efficacy of soft tissue augmentation around dental implants and in partially edentulous areas: a systematic review. *J Clin Periodontol*, *41 Suppl 15*, S77-91. https://doi.org/10.1111/jcpe.12220

Urban, I. A., Barootchi, S., Tavelli, L., & Wang, H. L. (2021). Inter-Implant Papilla Reconstruction via a Bone and Soft Tissue Augmentation: A Case Report with a Long-Term Follow-up. *Int J Periodontics Restorative Dent*, *41*(2), 169-175. https://doi.org/10.11607/prd.5280

Witkowski, S., Yajima, N. D., Wolkewitz, M., & Strub, J. R. (2012). Reliability of shade selection using an intraoral spectrophotometer. *Clin Oral Investig*, *16*(3), 945-949. https://doi.org/10.1007/s00784-011-0590-3

Witzel, R. F., Burnham, R. W., & Onley, J. W. (1973). Threshold and suprathreshold perceptual color differences. *J Opt Soc Am*, *63*(5), 615-625. https://doi.org/10.1364/josa.63.000615

Zetu, L., & Wang, H. L. (2005). Management of inter-dental/inter-implant papilla. *J Clin Periodontol*, *32*(7), 831-839. https://doi.org/10.1111/j.1600-051X.2005.00748.x

Zucchelli, G., Tavelli, L., McGuire, M. K., Rasperini, G., Feinberg, S. E., Wang, H. L., & Giannobile, W. V. (2020). Autogenous soft tissue grafting for periodontal and peri-implant plastic surgical reconstruction. *J Periodontol*, *91*(1), 9-16. https://doi.org/10.1002/jper.19-0350

Zucchelli G, T. L., Stefanini M, Barootchi S, Mazzotti C, Gori G, Wang HL. (2019). Classification of facial peri-implant soft tissue dehiscence / deficiencies at single implant sites in the esthetic zone. *J Periodontol*, *90*(10), 1116-1124.

Zweers, J., Thomas, R. Z., Slot, D. E., Weisgold, A. S., & Van der Weijden, F. G. (2014). Characteristics of periodontal biotype, its dimensions, associations and prevalence: a systematic review. *J Clin Periodontol*, *41*(10), 958-971. https://doi.org/10.1111/jcpe.12275

Tables

TABLE 1 Demographics

17 of the 33 implant crowns were cement-retained, and 16 of the 33 were screw-retained.

	Implants	**Teeth**
Patient Age (years)	65.5 years	65.5 years
Gender (M:F)	20:13	20:13
Number in study	33	33
Maxillary central incisor	6	6
Maxillary lateral incisor	9	9
Maxillary canine	1	1
Maxillary 1st premolar	10	10
Maxillary 2nd premolar	10	10
Probing depth (mm)	3.0 +/- 0.7	2.5 +/- 0.5

TABLE 2: Bone crest to papilla tip distance, and papilla tip to contact point

	Average papilla height[1], mm (SD)	**Average distance from papilla tip to contact point, mm (range)***	**Correlation, papilla height to papilla-contact distance**
Implant mesial papilla	2.7 (1.0)	0.1 (0 – 1.4)	-0.28
Tooth mesial papilla	2.6 (0.7)	0.4 (0 – 2.4)	-0.06
p-value, implant mesial papilla vs. tooth	0.72	0.04	-
Implant distal papilla	2.7 (0.9)	0.7 (0 – 1.5)	0.01
Tooth distal papilla	2.7 (0.8)	0.2 (0 – 1.7)	-0.13
p-value, implant distal papilla vs. tooth	0.74	0.65	-

1 = papilla height measured via ultrasonography from the interproximal bone crest to the papilla tip

* = range was used instead of standard deviation due to a non-normal distribution. (Majority of papillae had 0 space from contact point to papilla tip; using standard deviation resulted in a deviation larger than the average value).

TABLE 3: Buccal bone thickness, and buccal bone crest to free gingival/mucosal margin

	Average buccal bone thickness[1], mm (SD)	Average distance from buccal bone crest to free gingival/mucosal margin, mm (SD)
Implant	0.70 (0.3)	4.13 (1.5)
Tooth	0.63 (0.3)	2.9 (1.0)
p-value, implant vs. tooth	0.18	1.9×10^{-4}

1 = buccal bone thickness measured via ultrasonography 1mm apical to the buccal bone crest. Note that a limitation of ultrasonography is it cannot penetrate buccal bone by more than 1mm.

TABLE 4: Buccal soft tissue thicknesses: Implants vs. contralateral teeth

	Average free gingiva / mucosa thickness, mm (SD)	Average supracrestal adhesion / attachment thickness, mm (SD)	Average thickness at exact MGJ, mm (SD)	Average thickness of tissues 2mm beyond MGJ
Implant	2.0 (0.6)	2.3 (0.7)	1.9 (0.8)	1.8 (0.7)
Tooth	1.2 (0.3)	1.4 (0.5)	1.2 (0.5)	1.1 (0.5)
p-value[a] comparing implant vs. tooth values	1.7×10^{-8}	2.4×10^{-8}	5.31×10^{-5}	1.1×10^{-6}

a = p-value calculated by paired T-test

TABLE 5: Probing depth, buccal recession, BOP, and keratinized tissue width

	Average probing depth, mm (SD)	Average buccal recession, mm (SD)	Site-level % BOP average	Average KT width, mm (SD)
Implant	3.0 (0.7)	0.2	7.6%	3.3 (1.4)
Tooth	2.5 (0.5)	1.0	6.7%	3.5 (1.3)
p-value[a] comparing implant vs. tooth values	9.0×10^{-12}	n/a*	n/a*	0.52

* = Standard deviation exceeded the average, due to most implants and teeth having a measurement value of 0 and therefore, a non-normal distribution.

a = p-values calculated via paired T-test

TABLE 6: L* value correlation with tissue thickness

	Average L* value (SD)	Average tissue thickness[a], mm (SD)	Correlation, L* to tissue thickness	Linear regression p-value[b]
Implant	61.3 (9.8)	1.9 (0.7)	+0.16	0.37
Tooth	64.5 (9.4)	1.1 (0.4)	-0.07	0.78
p-value comparing implant vs. tooth values	0.008	3.4×10^{-7}	-	-

a = measured at the mucosal adhesion (in implants) and attached gingiva (in teeth)

b = p-value calculated via paired T-test

TABLE 7: Delta E (ΔE) classification of perceivable color differences

ΔE value	Perception level
Less than 1	Non-perceivable color difference.
1-2	Barely perceptible
2-10	Slightly perceptible
11-49	Perceptibly different, but still appear similar in color
100	Completely opposing colors on the color wheel

Table adapted from (Sensient, 2024).

TABLE 8: Delta E, to compare CIELAB color differences of implants vs. teeth

	Region analyzed			
	Free gingival/ mucosal margin	Supracrestal tissue adhesion / attachment	Mucogingival junction	Mucosa (apical to MGJ)
ΔE, implant vs. tooth	8.2	8.1	8.4	9.6

p-value[a] comparing implant vs. tooth values	0.96	0.82	0.48	0.16

a = p-value calculated via paired T-test

TABLE 9: Correlation analysis: Implant CIELAB L*a*b* and implant tissue thickness

	Implant free mucosal margin	Implant supracrestal tissue adhesion	Implant MGJ	Implant mucosa (apical to MGJ)
L* value to tissue thickness	+0.31	+0.16	+0.25	+0.16
a* value to tissue thickness	-0.37	-0.19	-0.19	+0.12
b* value to tissue thickness	-0.31	-0.06	+0.12	+0.02

TABLE 10: Correlation analysis: Tooth CIELAB L*a*b* and tooth tissue thickness

	Tooth free gingival margin	Tooth supracrestal tissue attachment	Tooth MGJ	Tooth mucosa (apical to MGJ)
L* value to tissue thickness	+0.12	-0.02	-0.04	-0.05
a* value to tissue thickness	+0.13	+0.00	-0.09	+0.31
b* value to tissue thickness	+0.11	+0.27	+0.17	+0.38

TABLE 11: ΔL*, a*, b* for every 1mm ST thickness increase

	Implant free mucosal margin	Tooth free gingival margin	Implant supracrestal tissue adhesion	Tooth supracrestal tissue adhesion
L*	+4.99 +/- 2.81 p = 0.09	+2.10 +/- 5.14 p = 0.68	+2.38 +/- 2.61 p = 0.37	-1.04 +/- 3.69 p = 0.78
a*	-3.69 +/- 1.64 p = 0.032	+2.092 +/- 2.95 p = 0.48	-1.70 +/- 1.55 p = 0.28	+0.03 +/- 2.20 p = 0.99
b*	-1.87 +/- 1.02 p = 0.13	+0.77 +/- 2.06 p = 0.71	-0.11 +/- 1.06 p = 0.92	+1.92 +/- 1.35 p = 0.16

TABLE 12: Ultrasonography: Power and Perfusion comparison

	Average perfusion (SD)	Average Power (SD)
Implant	0.07 (0.16)	0.04 (0.03)
Tooth	0.08 (0.18)	0.04 (0.03)
p-value[a] comparing implant vs. tooth values	0.4	0.44

a = p-value calculated via paired T-test

TABLE 13: Characterization of the healthy peri-implant mucosa.

	Average value of this study, mm (SD)
Distance of buccal bone crest to free gingival margin	4.13 (1.5)
Buccal soft tissue thickness	~0.8 mm thicker than contralateral teeth
Buccal bone thickness	0.7 (0.3)
KTW	3.3 (1.4)
BOP	7.6%
Papilla heights	Mesial papilla: 2.7 (1.0) Distal papilla: 2.7 (0.9)
Ultrasonographic power	0.04 (0.03)
Ultrasonographic perfusion	0.07 (0.16)
Stippling	Can be present or absent

Contour	Minimal recession
Form	Scalloped gingival margins
Consistency	Resilient; rebounds to pressure
Color	Coral pink

Table 14: ΔE comparing tooth vs. implant zones

	FG	A	MGJ	M	MPAP	DPAP
ΔE of implant vs. tooth's same zone	3.80734393	3.46396907	2.863756611	2.010760767	3.585118721	2.853959921
Stdev	6.14106618	6.65180101	6.64636826	6.308054728	5.357097	5.8782393
paired ttest	0.09130597	0.24350763	0.047773809	0.643310097	0.259038951	0.022488511

Table 15: ΔE comparing implant zones to each other

	FG-A	FG-MGJ	FG-M	FG-MPAP	FG-DPAP	A-MGJ	A-M	A-MPAP	A-DPAP	MGJ-M	MGJ-MPAP	MGJ-DPAP	M-MPAP	M-DPAP	MPAP-DPAP
Average ΔE	2.92	8.26	16.15	8.12	6.04	7.20	15.72	8.72	6.70	10.01	9.60	10.01	15.60	16.05	7.46
Std ΔE	1.77	4.37	8.35	4.66	3.81	4.20	8.39	4.69	3.60	5.17	5.40	4.76	8.74	8.89	3.76
paired ttest	0.73	2.64871E-05	3.54E-10	0.41	0.39	2.65512E-06	1.98211E-10	0.49	0.32	8.74405E-10	0.00044839	0.01	8.02888E-11	7.94091E-09	0.07

* FG: Free mucosal margin
A: Supracrestal tissue adhesion
MGJ: Mucogingival junction
M: Mucosa apical to MGJ
MPAP: Mesial papilla measured above papilla base (where the base is the line drawn from zenith to zenith of adj. teeth)
DPAP: Distal papilla measured above papilla base (where the base is the line drawn from zenith to zenith of adj. teeth)

Table 16: ΔE comparing tooth zones to each other

ΔE comparing tooth zones to each other

	FG -A	FG-MGJ	FG-M	FG-MPAP	FG-DPAP	A-MGJ	A-M	A-MPAP	A-DPAP	MGJ-M	MGJ-MPAP	MGJ-DPAP	M-MPAP	M-DPAP	MPAP-DPAP
Average ΔE	3.25080337	7.921320844	15.17496979	3.733665629	5.494456507	7.609435638	15.70178933	5.052726893	6.366428326	9.482462927	8.649094888	8.429111421	15.5722423	14.7847811	6.234203825
STD	2.82989154	4.388686844	9.441877514	1.785107246	2.946190728	4.283632168	9.508180337	2.775497597	3.19894261	5.578237836	4.678321686	4.508155618	9.873692788	8.367600535	3.830164765
Paired ttest	0.96	4.60929E-09	1.17695E-12	0.04	1.28031E-05	2.7817E-11	9.18074E-12	0.19	4.98105E-05	3.87535E-09	4.23308E-10	0.03	5.66493E-13	2.8439E-08	4.41891E-06

* FG: Free gingival margin
A: Supracrestal tissue attachment
MGJ: Mucogingival junction
M: Mucosa apical to MGJ
MPAP: Mesial papilla measured above papilla base (where the base is the line drawn from zenith to zenith of adj. teeth)
DPAP: Distal papilla measured above papilla base (where the base is the line drawn from zenith to zenith of adj. teeth)

Figures

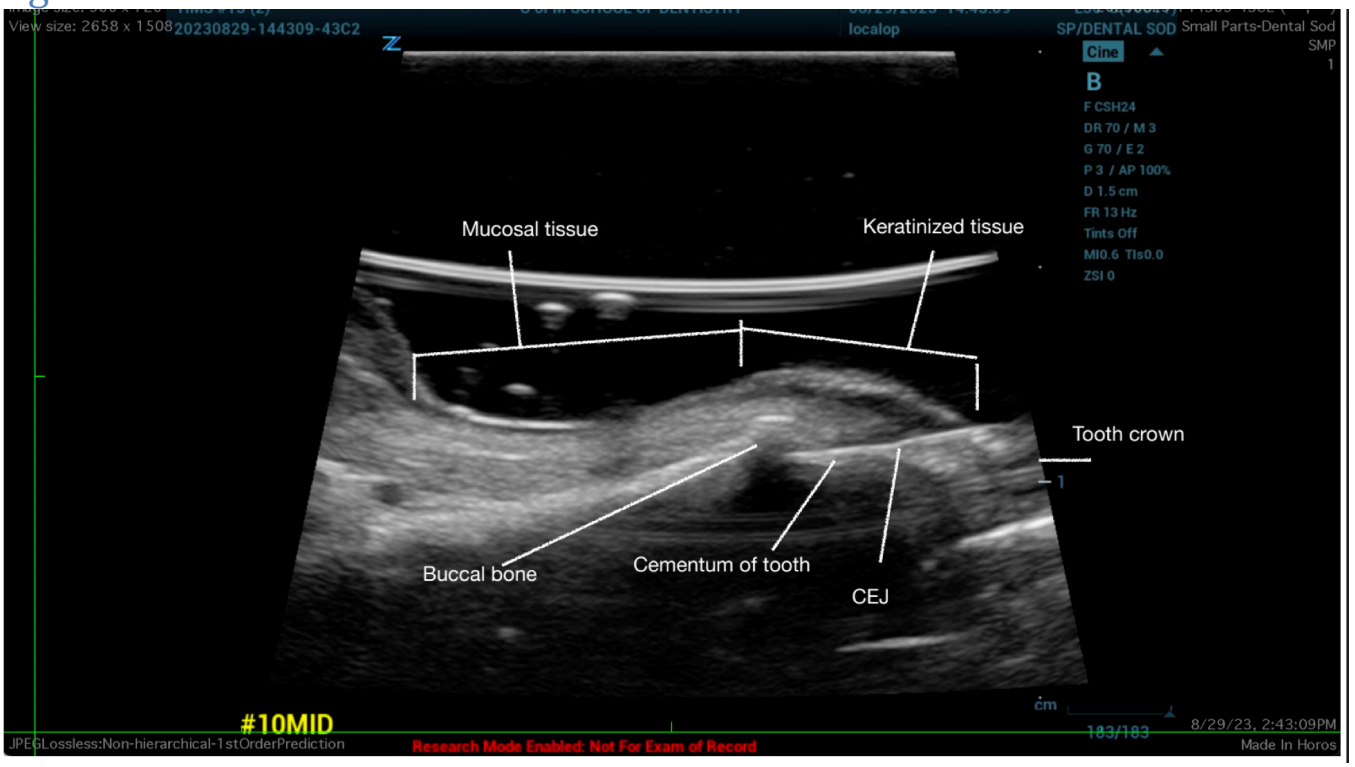

Figure 1. Annotated ultrasound image showing the buccal sagittal "slice" of a tooth. Annotations denote key anatomic landmarks.

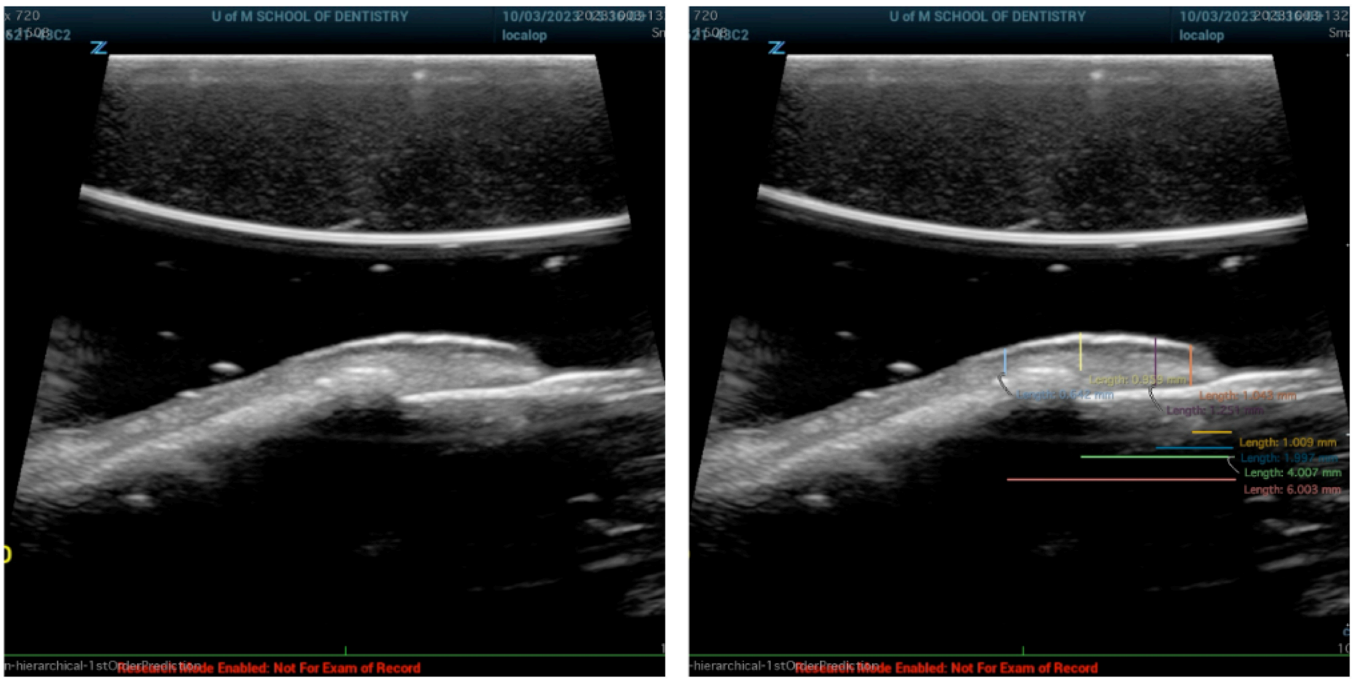

Figure 2. (Left) A ultrasonographic sagittal “slice” image of a natural tooth. (Right) Example of the linear measurement data extracted via the measurement function in Horos software.

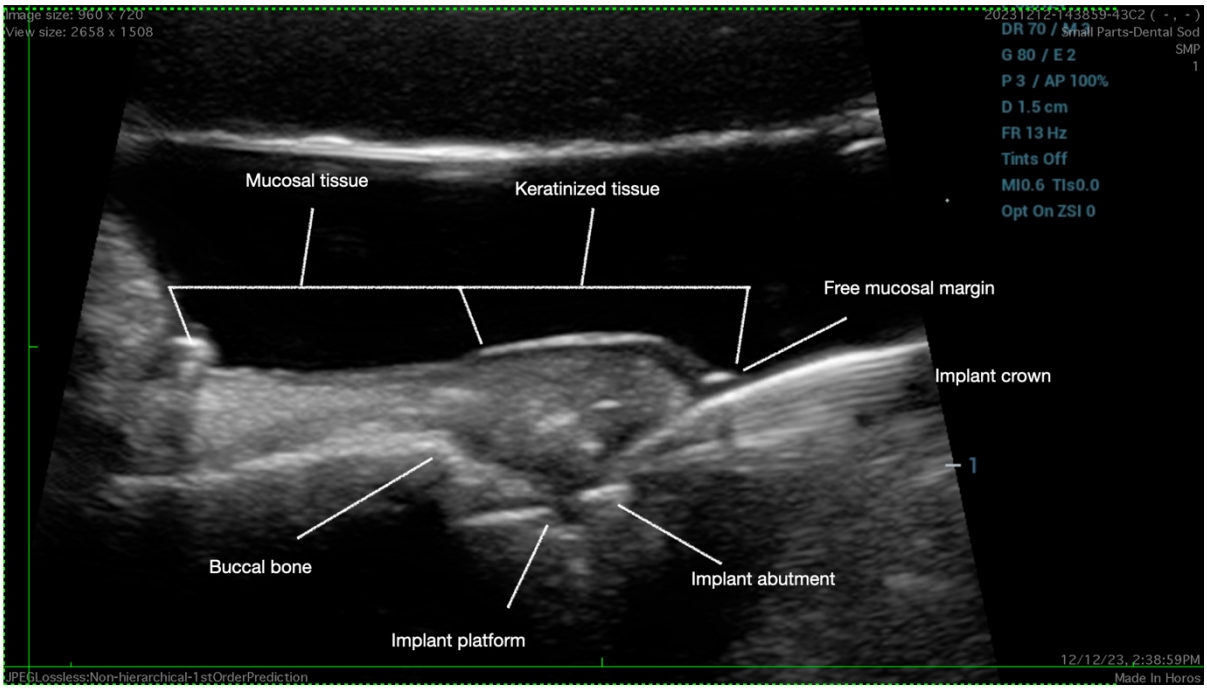

Figure 3. Annotated ultrasound image showing the buccal sagittal “slice” of an implant. Annotations describe key anatomic landmarks.

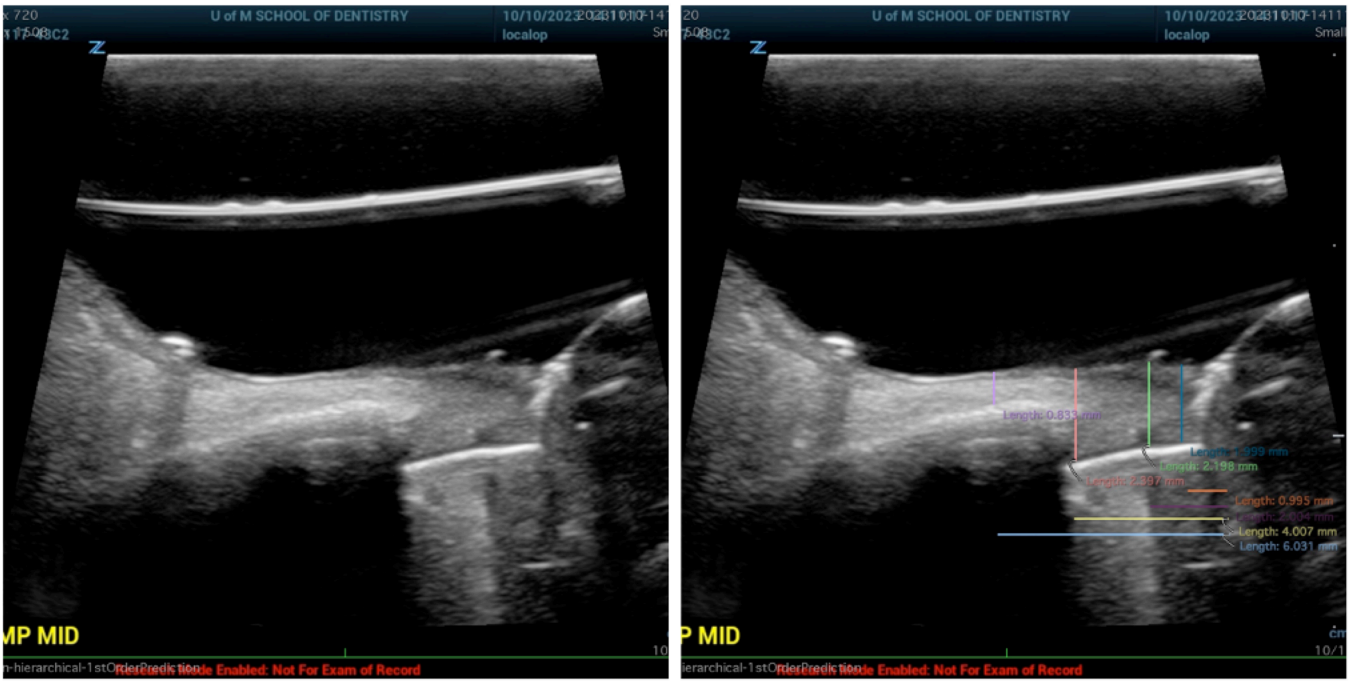

Figure 4. (Left) Ultrasonographic sagittal "slice" image of an implant. (Right) Linear measurement data extraction from the image using the measurement function in Horos software.

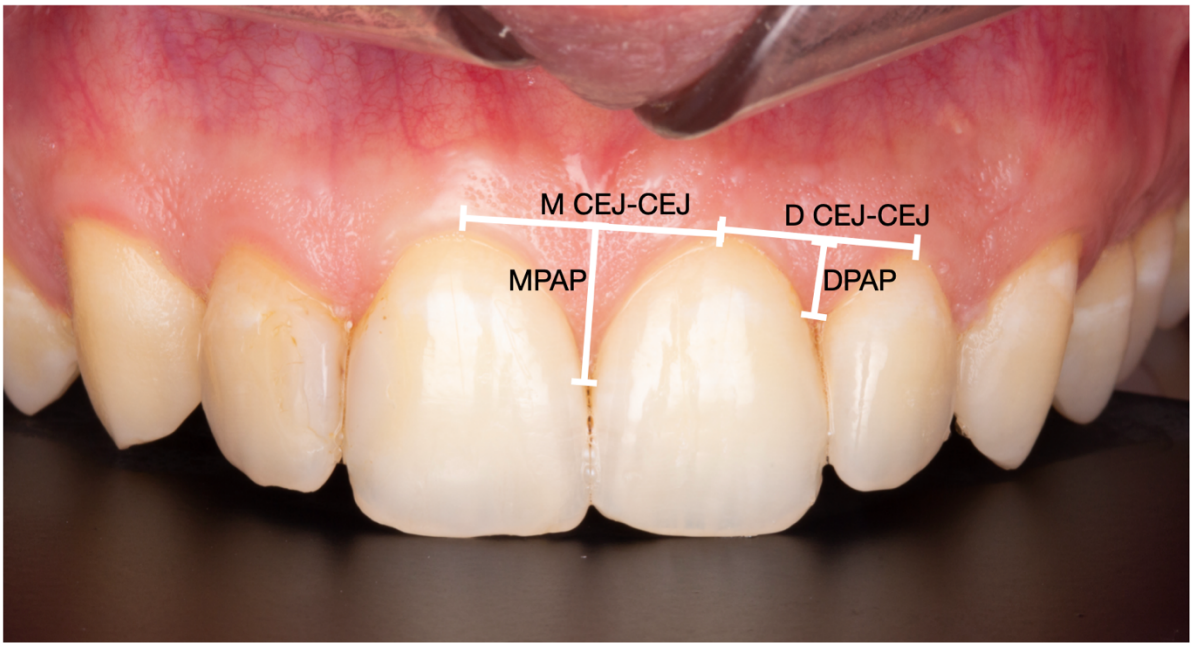

Figure 5: Diagram describing clinical measurements. D CEJ-CEJ: Distal papilla base (aka "papilla width") measured from gingival zeniths of adjacent teeth. DPAP height: Height of the distal papilla as measured from D CEJ-CEJ to the papilla tip. Similar measurement landmarks are used for M CEJ-CEJ, MPAP height.

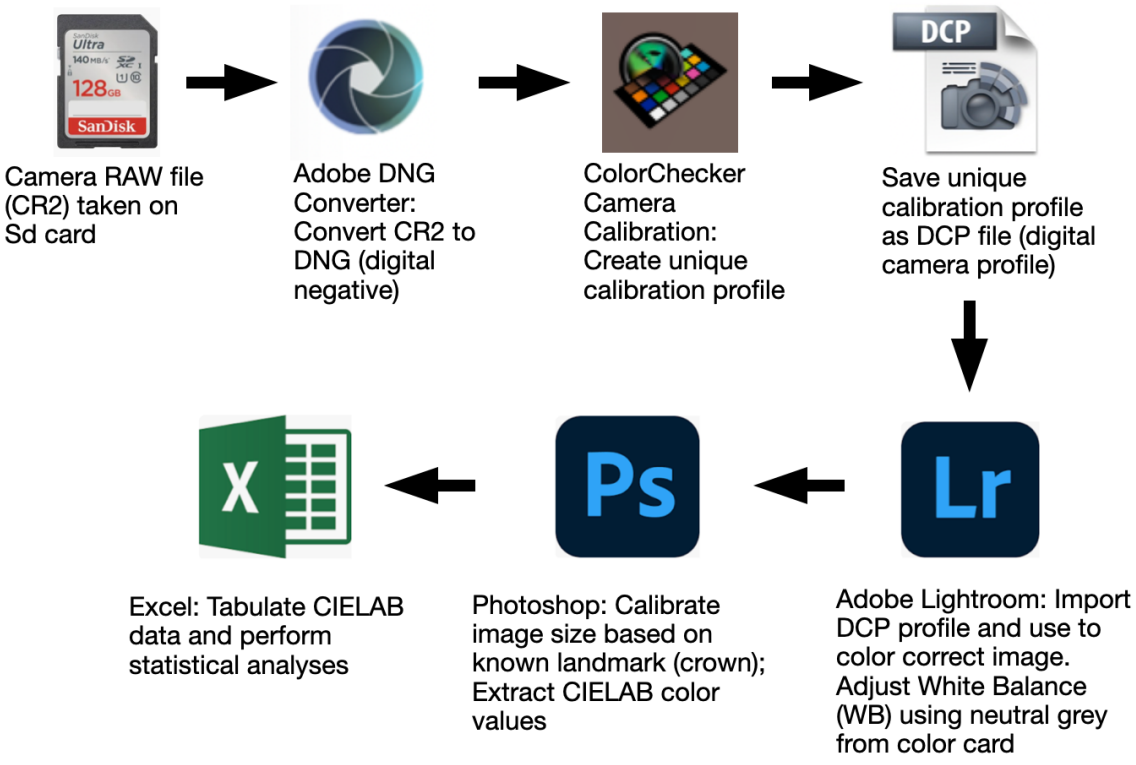

Supplemental Figure 1. Digital workflow for the conversion of camera RAW files to color calibrated images allowing the extraction of color data. The ColorChecker calibration card allowed standardization of the environmental lighting and white balance levels between cases.

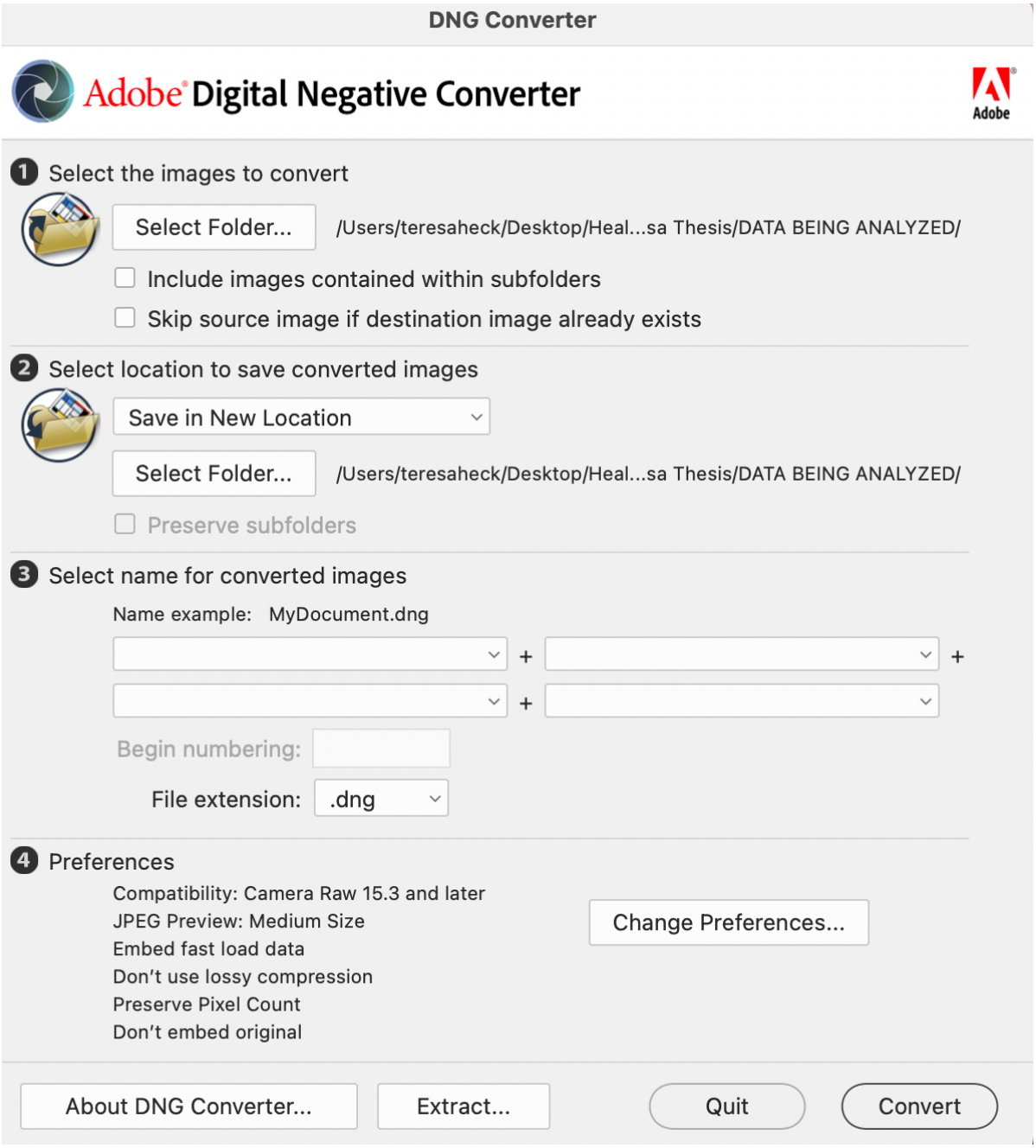

Supplemental Figure 2. Example of Adobe Digital Negative Converter. This software allows lossless conversion of the camera RAW files to DNG (digital negative) format, which can then be further processed in photoediting software.

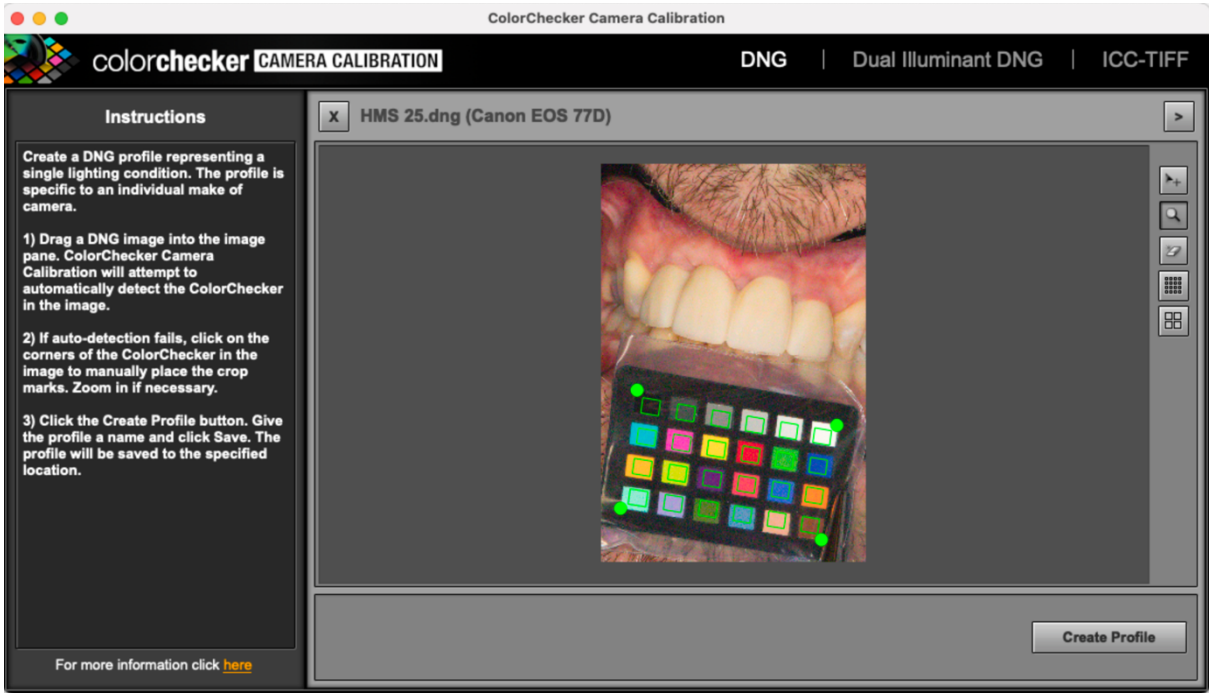

Supplemental Figure 3. Screenshot of the ColorChecker Camera Calibration software. This software utilizes the ColorChecker Nano calibration card to create a color correction profile to standardize the environmental lighting of each image.

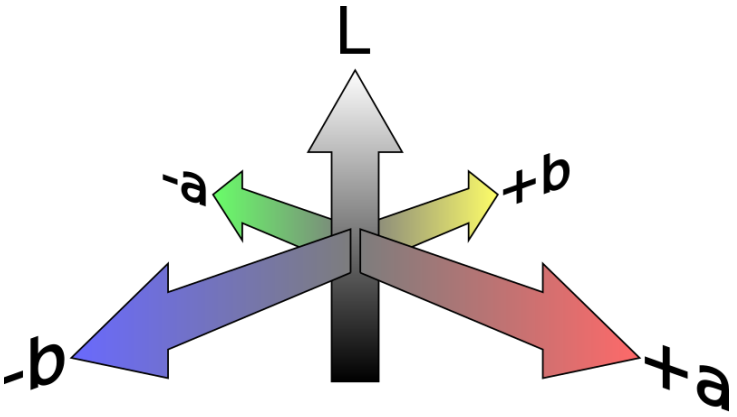

Supplemental Figure 4: A diagram describing the color axes of the CIE L*, a*, and b* values.

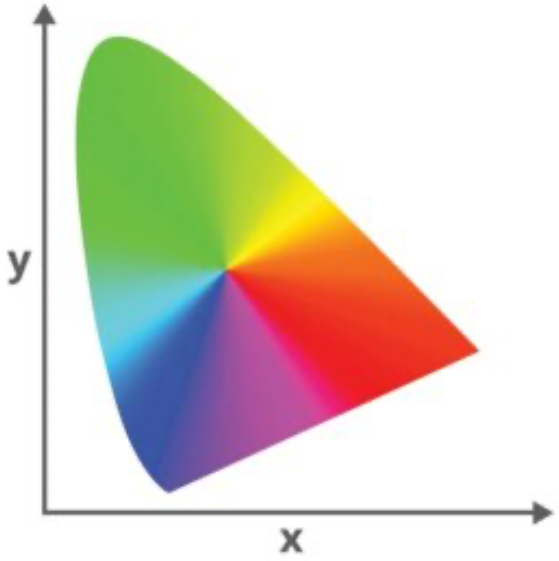

Supplemental Figure 5: Another variation of the CIELAB colorspace map. Source: (Datacolor, 2024)

Supplemental Figure 6: Characteristics of implants included in the study.

	A	B	C	D	E	F	G
1	HMS#	Implant#	Implant brand	BL or TL?	Diameter	Placement date	Prosthesis date
2	1	13	Straumann	BL	4.1	6/16/06	1/5/07
3	2	10	Zimmer TSV	TL	3.7	9/30/22	3/30/23
4	3	5	Zimmer TSV	TL	3.1	10/20/17	3/1/19
5	4	8	Straumann	BL	4.1	3/9/22	9/14/22
6	5	13	Zimmer TSV	TL	4.1	1/29/15	5/16/22
7	6	13	Straumann	BL	4.1	7/27/22	3/23/23
8	7	8	Straumann BLX	BL	3.75	7/19/22	12/8/22
9	8	12	Biomet 3i	BL	4.1	2021	2021
10	9	4	Zimmer TSV	TL	4.1	5/16/02	10/1/02
11	10	5	Biohorizon	TL	3.8	8/4/17	12/5/17
12	11	4	Zimmer TSV	TL	3.7	12/1/17	5/10/19
13	12	7	Nobel Biocare	BL	3.5	2016	2016
14	13	4	Zimmer TSV	TL	3.7	1/25/18	5/14/18
15	14	8	Straumann BLX	BL	3.75	2012	2012
16	15	5	Zimmer TSV	TL	3.7	2/1/23	9/11/23
17	16	9	Straumann BLT	BL	4.1	2015	2015
18	17	10	Straumann BLT	BL	3.3	2/26/21	12/8/21
19	18	7	Straumann	BL	3.3	2008	2008
20	19	11	Zimmer TSV	TL	4.1	2021	2021
21	20	10	Camlog Root-Line J series	TL	3.8	2008	2008
22	21	13	Zimmer TSV	TL	3.7	4/8/22	10/4/22
23	22	10	Straumann BLT	BL	4.1	2017	2017
24	23	11	Straumann	BL	4.1	2014	2014
25	24	10	Straumann ITI	BL	3.3	2008	2008
26	25	4	Zimmer TSV	TL	3.7	2/1/22	9/15/22
27	26	10	Straumann	BL	3.75	2014	2014
28	27	10	Zimmer TSV	TL	3.7	2021	2021
29	28	8	Neobiotech	BL	4	2/16/17	8/10/17
30	29	4	Zimmer TSV	TL	4.1	2019	2019
31	30	5	Straumann BLX	BL	3.75	2008	2008
32	31	12	Zimmer TSV	TL	4.1	2012	2012
33	32	4	Zimmer TSV	TL	3.7	2/1/19	10/10/19
34	33	11	Straumann BLT	BL	4.1	2018	2018
35				Total BL: 18			
36				Total TL: 15			

ANCOVA

Sushwarya

2024-08-01

R Markdown

This is an R Markdown document. Markdown is a simple formatting syntax for authoring HTML, PDF, and MS Word documents. For more details on using R Markdown see http://rmarkdown.rstudio.com.

When you click the **Knit** button a document will be generated that includes both content as well as the output of any embedded R code chunks within the document. You can embed an R code chunk like this:

Note that the `echo = FALSE` parameter was added to the code chunk to prevent printing of the R code that generated the plot.

```
library(readxl)
implant_data <- read_excel("for ANCOVA analysis.xlsx",
    sheet = "Implant variables")
View(implant_data)
```

```
head(implant_data)
```

```
## # A tibble: 6 × 20
##   `Patient #` Implant.deltaE.of.FG Implant.deltaE.of.A `Implant deltaE of MGJ`
##         <dbl>                <dbl>               <dbl>                   <dbl>
## 1           1                 71.0                73.6                    77.2
## 2           2                 78.9                78.9                    73.4
## 3           3                 73.3                75.3                    73.9
## 4           4                 70.9                72.1                    70.0
## 5           5                 73.4                71.8                    69.8
## 6           6                 79.2                79.5                    76.0
## # ℹ 16 more variables: `Implant delta E of M` <dbl>,
## #   `Implant delta E of MPAP` <dbl>, `Implant deltaE of DPAP` <dbl>,
## #   Implant.ST.4mm.from.FGM <dbl>,
## #   `Implant MPapilla height (from crest)` <dbl>,
## #   `Implant DPapilla height (from crest)` <dbl>,
## #   `Implant tip of Buccal bone distance from FGM` <dbl>,
## #   `Implant M CEJ-CEJ` <dbl>, `Implant M PapH` <dbl>, …
```

#Let's assume you want to analyze the effect of Implant.deltaE.of.FG (as the dependent variable) with Implant.deltaE.of.A as the independent variable and Implant.ST.4mm.from.FGM as the covariate. You can adjust the variables according to your analysis needs

```
ancova_model <- aov(Implant.ST.4mm.from.FGM ~ Implant.deltaE.of.A *Implant.deltaE.of.FG , data = implant_data)

summary(ancova_model)
```

```
##                                       Df Sum Sq Mean Sq F value Pr(>F)
## Implant.deltaE.of.A                    1  1.054  1.0540   2.410  0.131
## Implant.deltaE.of.FG                   1  0.253  0.2532   0.579  0.453
## Implant.deltaE.of.A:Implant.deltaE.of.FG  1  1.311  1.3107   2.997  0.094 .
## Residuals                             29 12.682  0.4373
## ---
## Signif. codes:  0 '***' 0.001 '**' 0.01 '*' 0.05 '.' 0.1 ' ' 1
```

```
# Plot residuals
plot(ancova_model, which = 1)
```

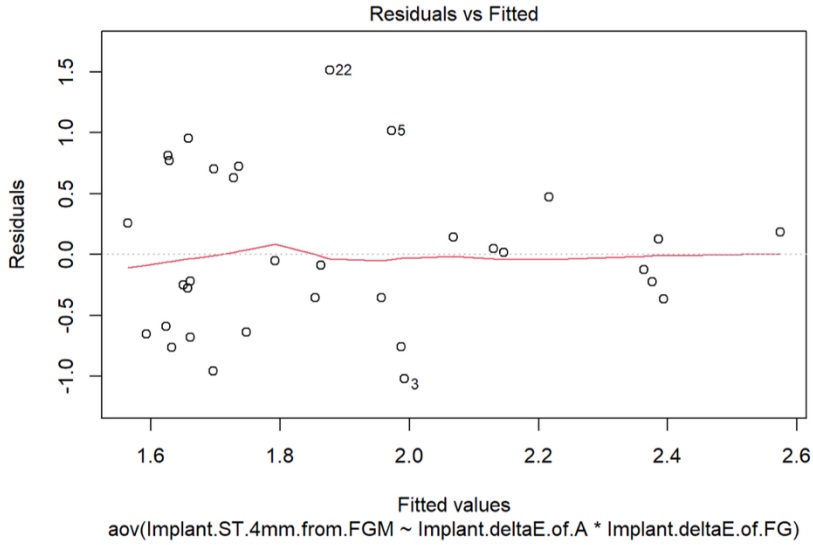


```
# Check for homogeneity of regression slopes
interaction_model <- aov(Implant.ST.4mm.from.FGM ~ Implant.deltaE.of.A *Implant.deltaE.of.FG , data = implant_dat
a)
summary(interaction_model)
```

```
##                                        Df Sum Sq Mean Sq F value Pr(>F)
## Implant.deltaE.of.A                     1  1.054  1.0540   2.410  0.131
## Implant.deltaE.of.FG                    1  0.253  0.2532   0.579  0.453
## Implant.deltaE.of.A:Implant.deltaE.of.FG  1  1.311  1.3107   2.997  0.094 .
## Residuals                              29 12.682  0.4373
## ---
## Signif. codes:  0 '***' 0.001 '**' 0.01 '*' 0.05 '.' 0.1 ' ' 1
```

Supplemental Figure 7: A statistical output following ANOVA and ANCOVA analyses of the obtained data. No significant findings could be found.

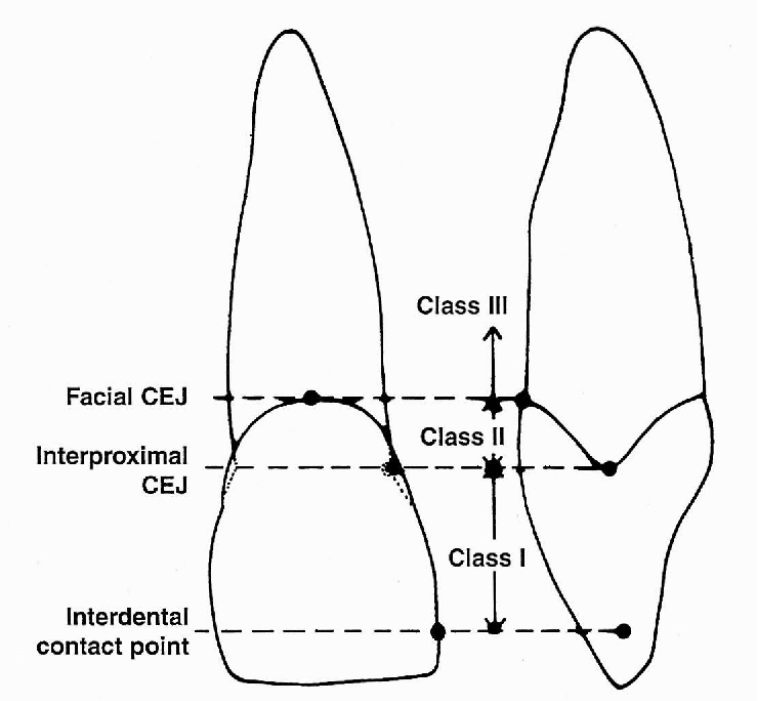

Figure 4: Diagram from the original Nordland & Tarnow 1998 classification, describing the three papilla classifications. (Image source: Nordland WP, Tarnow DP. A classification system for loss of papillary height. J Periodontol. 1998 Oct;69(10):1124-6. doi: 10.1902/jop.1998.69.10.1124. PMID: 9802711.)

Class I: Papilla tip is present between the contact point and the interproximal CEJ.

Class II: The papilla tip is located between the facial CEJ and interproximal CEJ.

Class III: The papilla is located apical to the facial CEJ of the tooth.

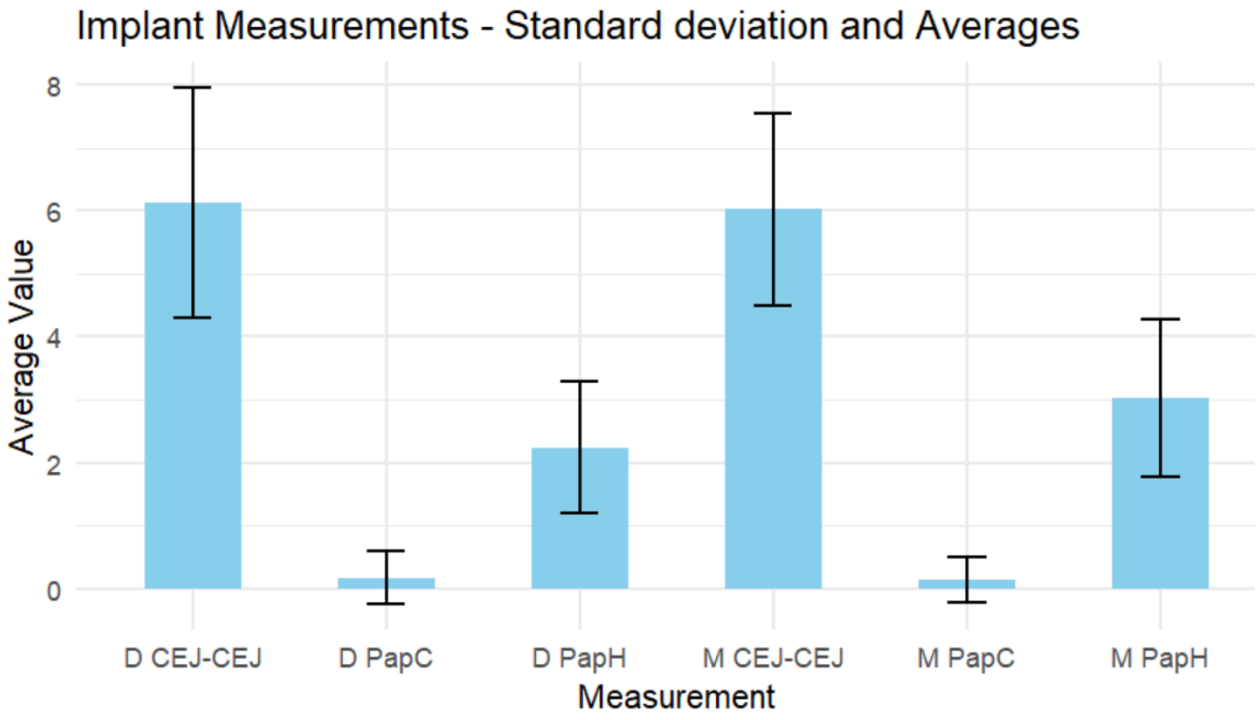

Figure 5a: Box-and-whisker plot illustrating the average values of implant measurements. D CEJ-CEJ: Distal papilla base (aka, “papilla width”) as measured from buccal zenith CEJ to the adjacent buccal zenith CEJ. D PapC: Distal papilla tip to contact point. D PapH: Distal papilla height. M CEJ-CEJ: Mesial papilla base (aka, “papilla width”) as measured from buccal zenith CEJ to the adjacent buccal zenith CEJ. M PapC: Mesial papilla tip to contact point. M PapH: Mesial papilla height.

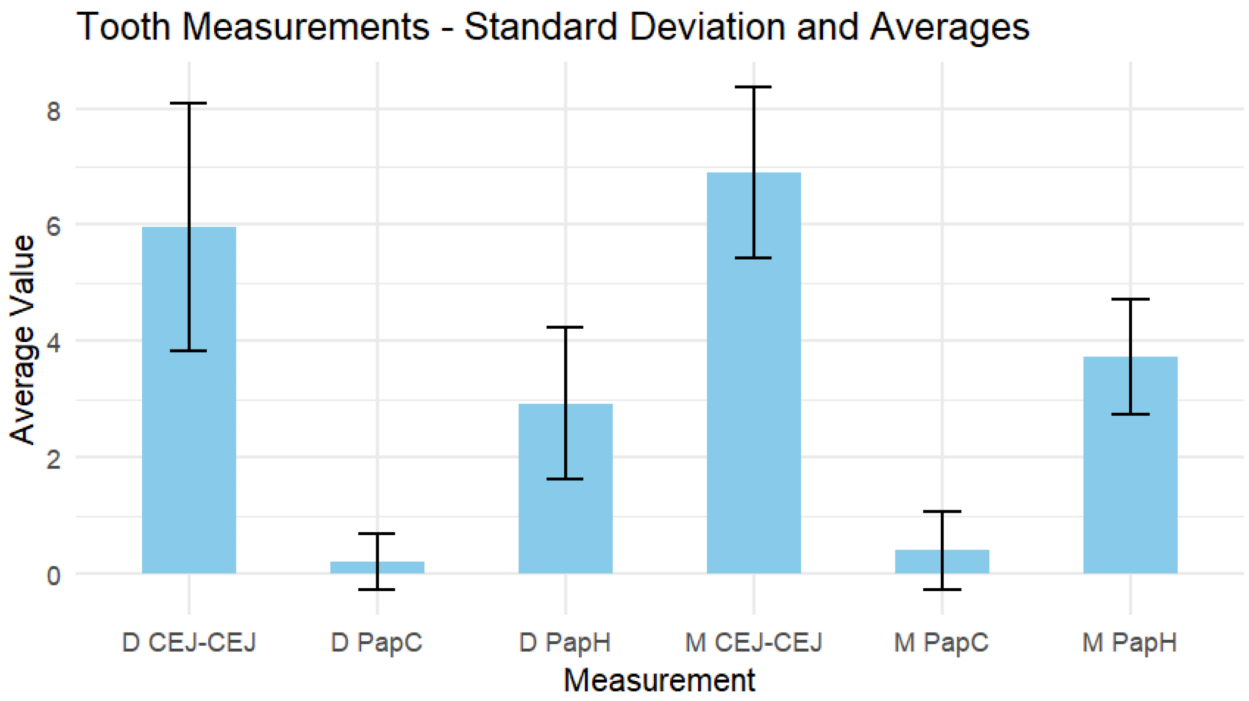

Figure 6: Box-and-whisker plot illustrating the average values of tooth measurements. D CEJ-CEJ: Distal papilla base as measured from buccal zenith CEJ to the adjacent buccal zenith CEJ. D PapC: Distal papilla tip to contact point. D PapH: Distal papilla height. M CEJ-CEJ: Mesial papilla base (aka, "papilla width") as measured from buccal zenith CEJ to the adjacent buccal zenith CEJ. M PapC: Mesial papilla tip to contact point. M PapH: Mesial papilla height.

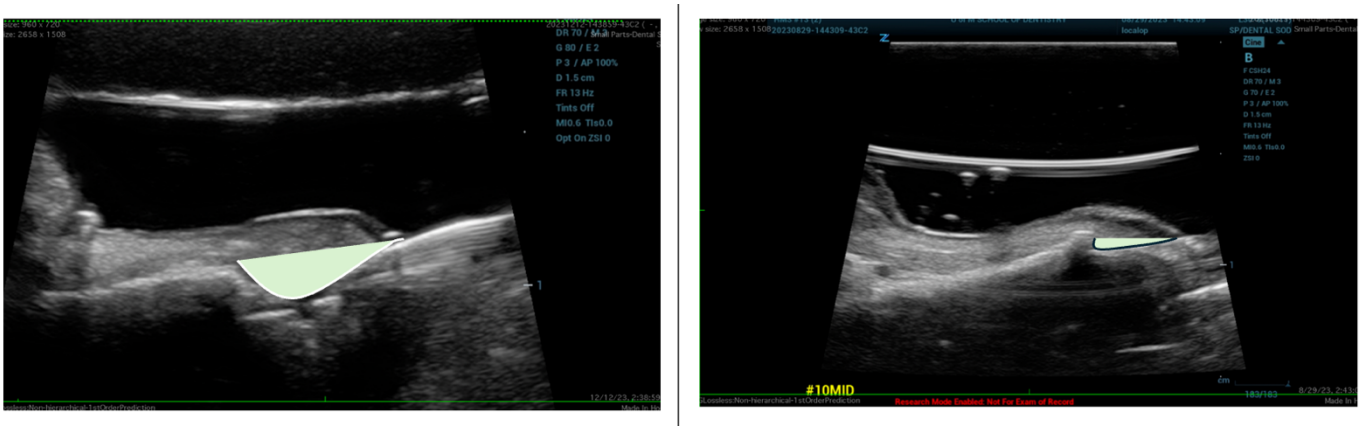

Figure 7: Subgingival buccal profile comparison between an implant (left) and natural tooth (right). The pale green shape indicates the concavity present between the CEJ and

the buccal bone crest. Original images were obtained via ultrasonography.

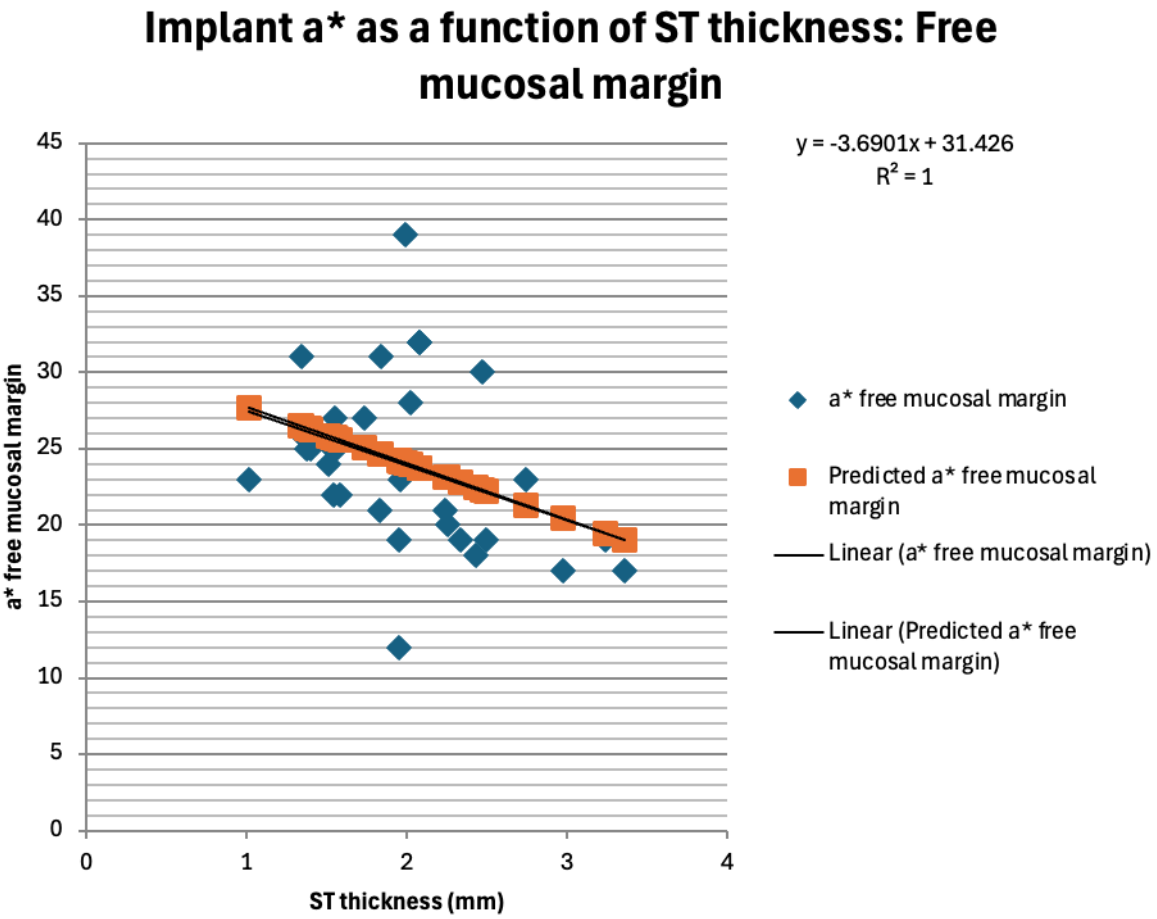

Figure 8: Linear regression analysis of scatter plot data, showing a negative relationship between implant a* value and free mucosal margin thickness.

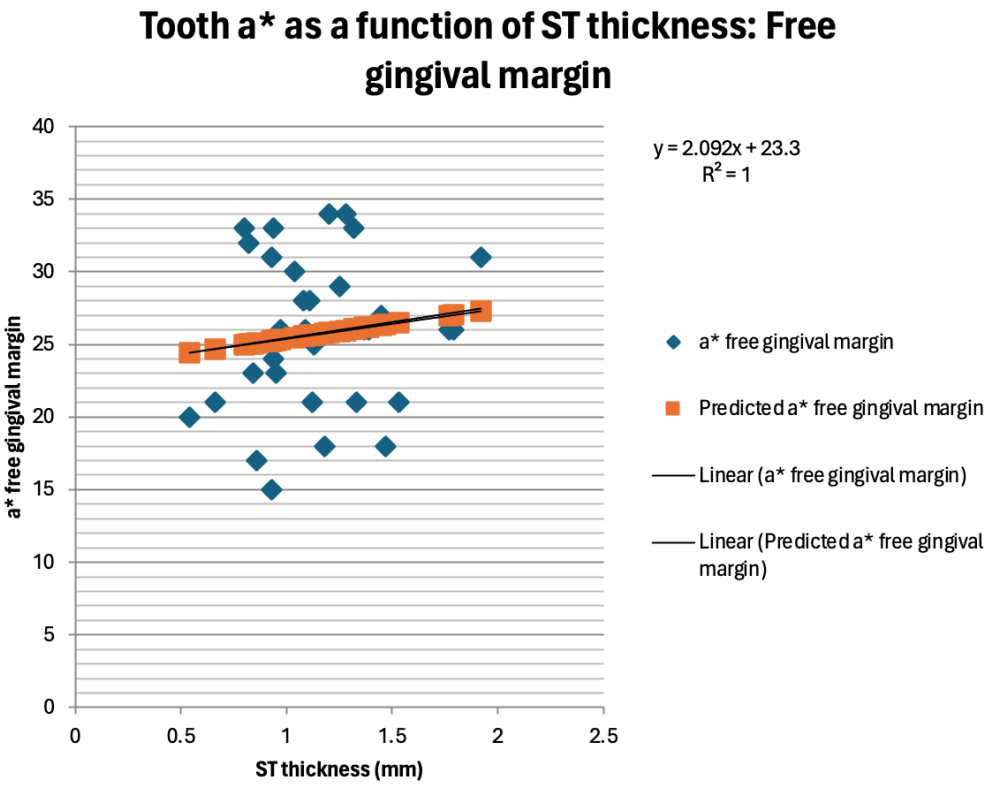

Figure 9: Linear regression analysis of scatter plot data, showing a positive relationship between tooth a* value and free gingival margin thickness.

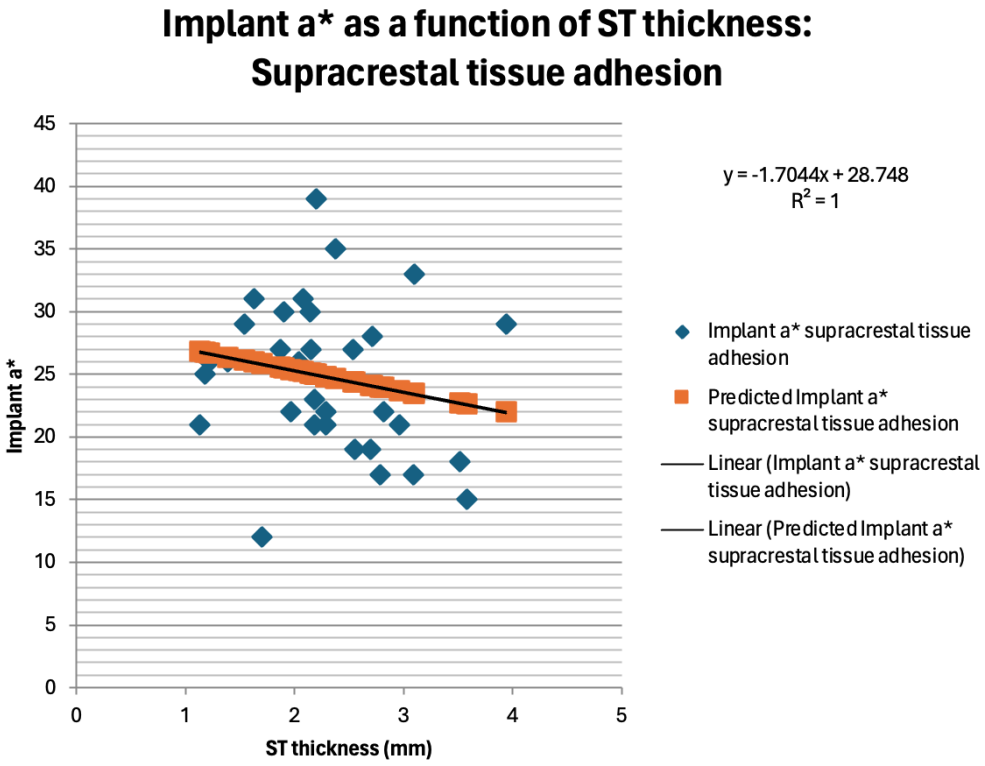

Figure 10: Linear regression analysis of scatter plot data, showing a negative relationship between implant a* value and the thickness of the supracrestal tissue adhesion.

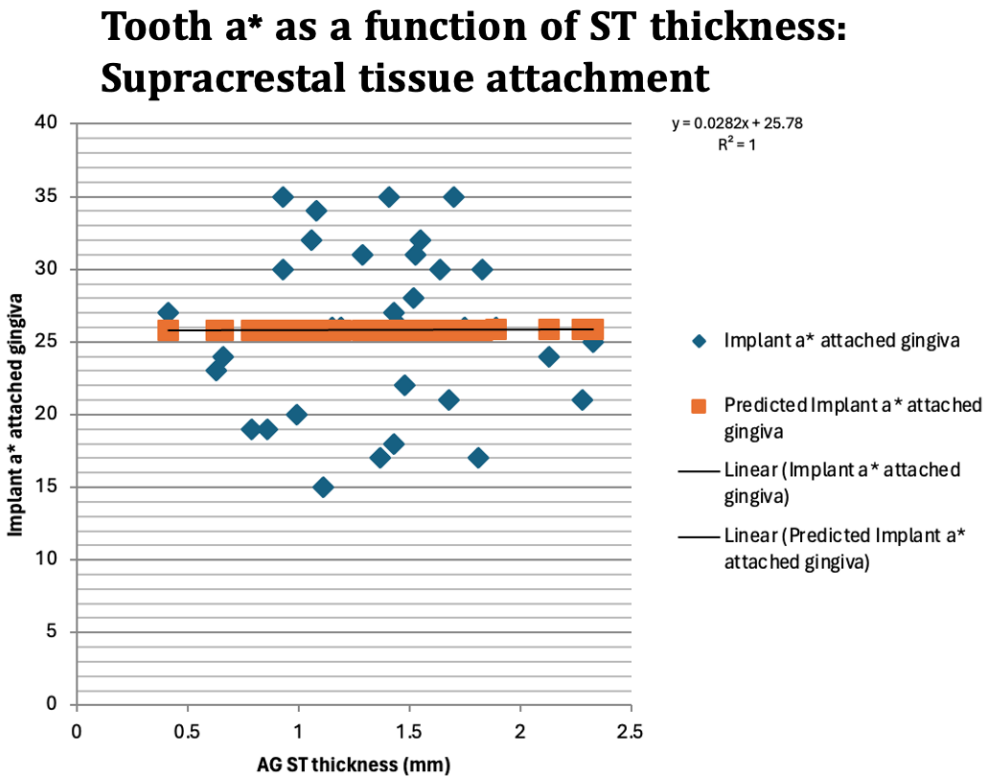

Figure 11: Linear regression analysis of scatter plot data, showing a weakly positive relationship between tooth a* value and the thickness of the supracrestal tissue attachment.

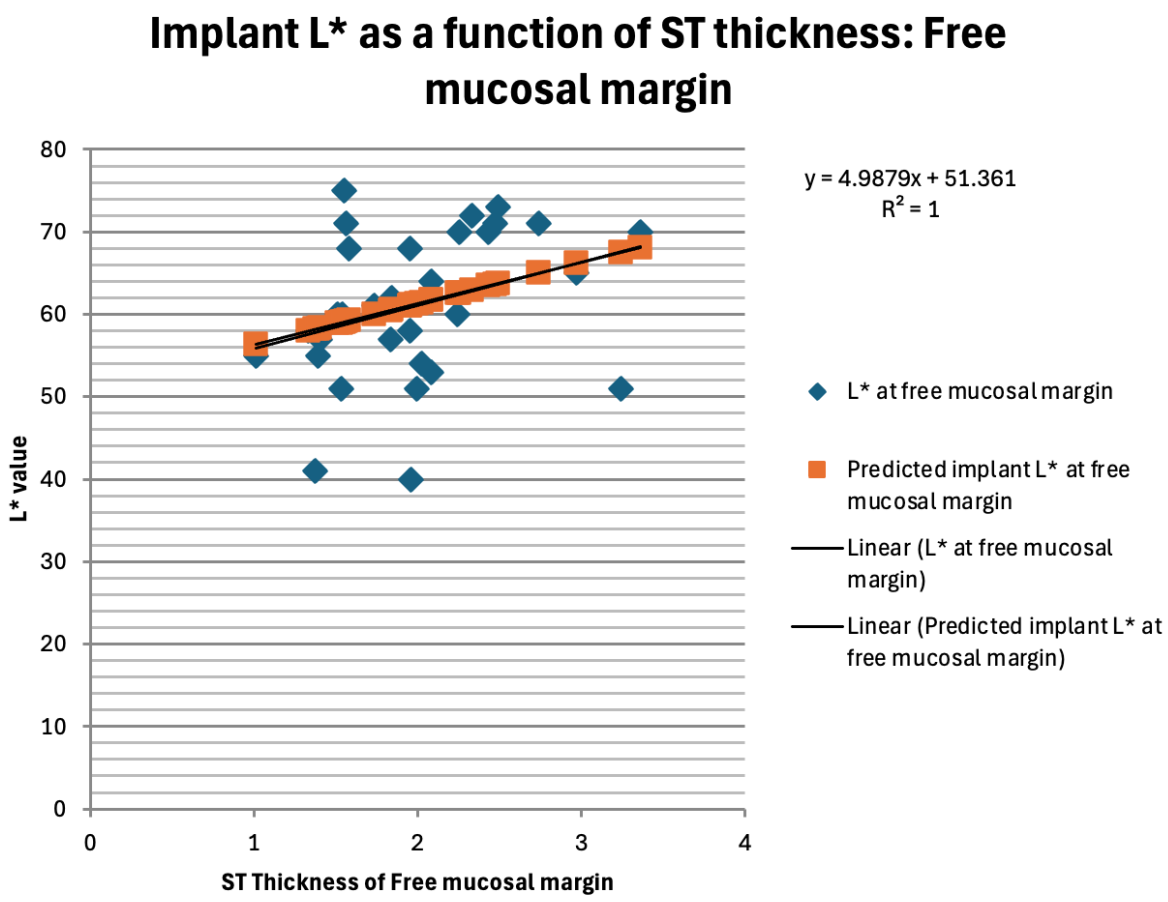

Figure 12: Linear regression analysis of scatter plot data, showing a positive relationship between implant L* value and the thickness of the free mucosal margin.

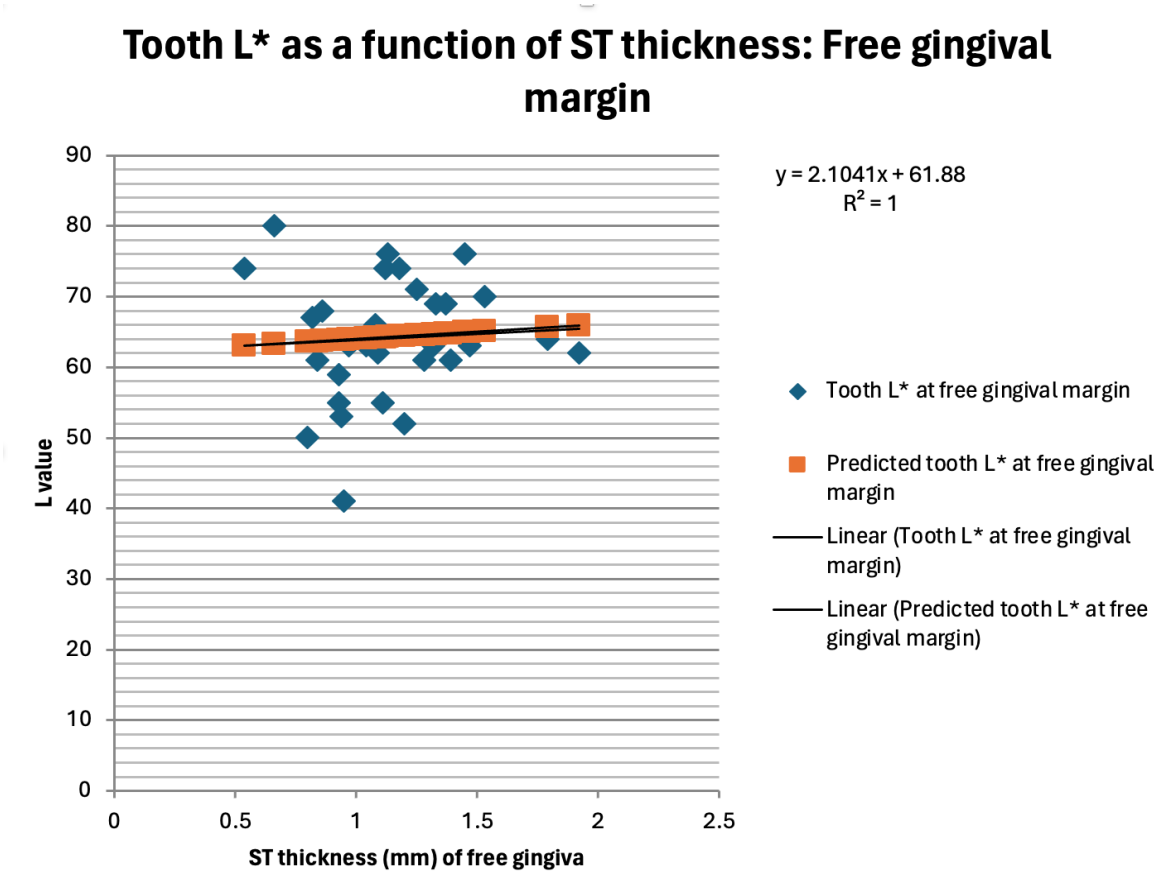

Figure 13: Linear regression analysis of scatter plot data, showing a weakly positive relationship between tooth L* value and thickness of the free gingival margin.

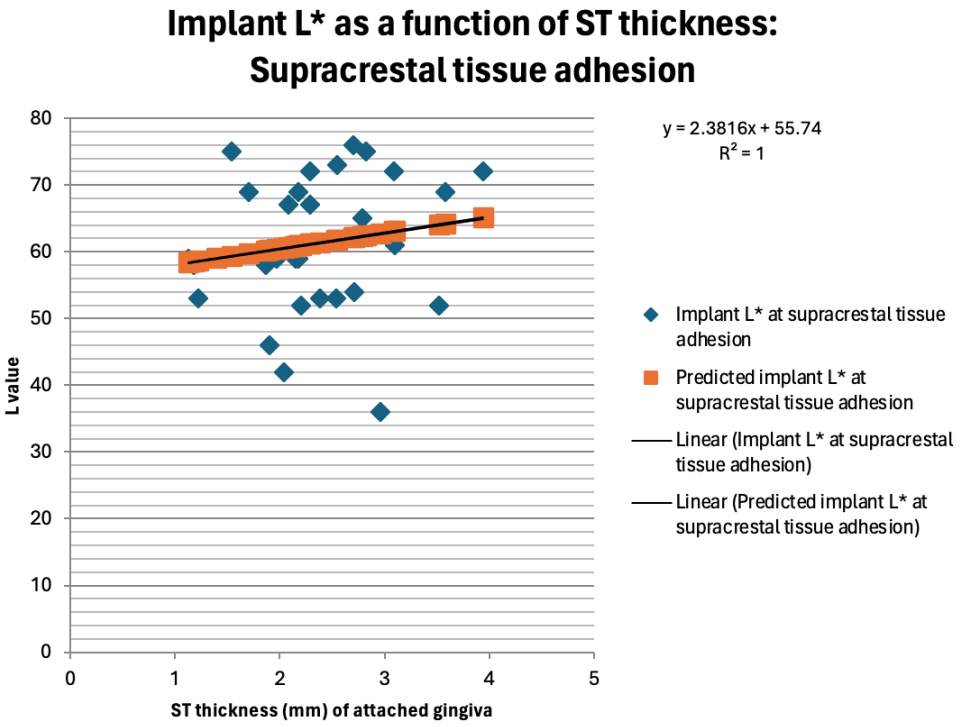

Figure 14: Linear regression analysis of scatter plot data, showing a positive relationship between implant L* value and thickness of the supracrestal tissue adhesion.

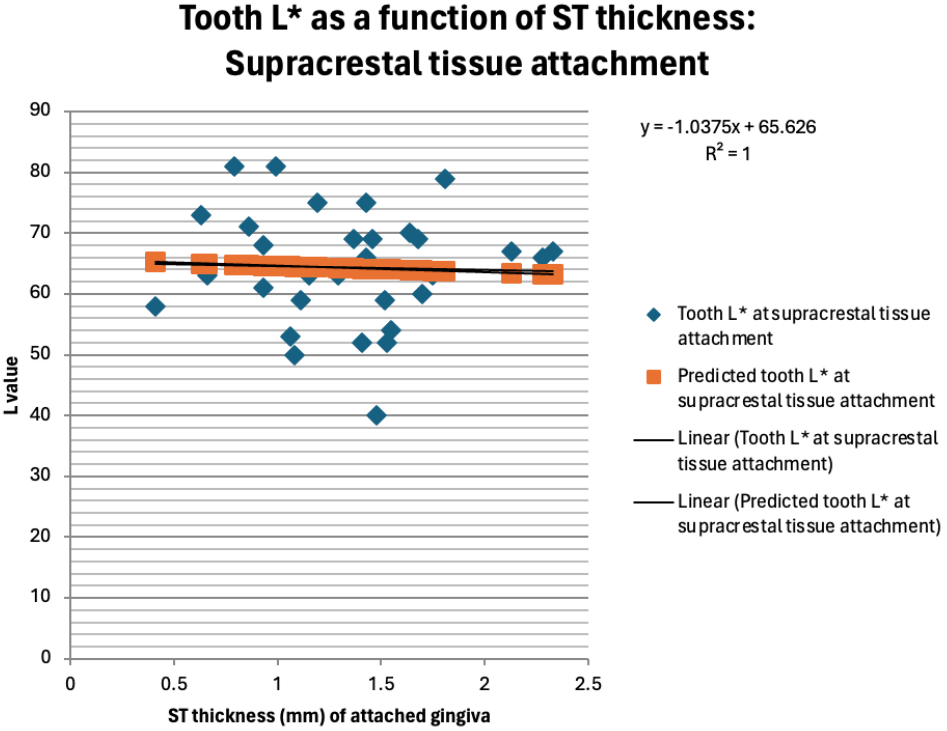

Figure 15: Linear regression analysis of scatter plot data, showing a very weakly negative relationship between tooth L* value and thickness of the supracrestal tissue attachment.

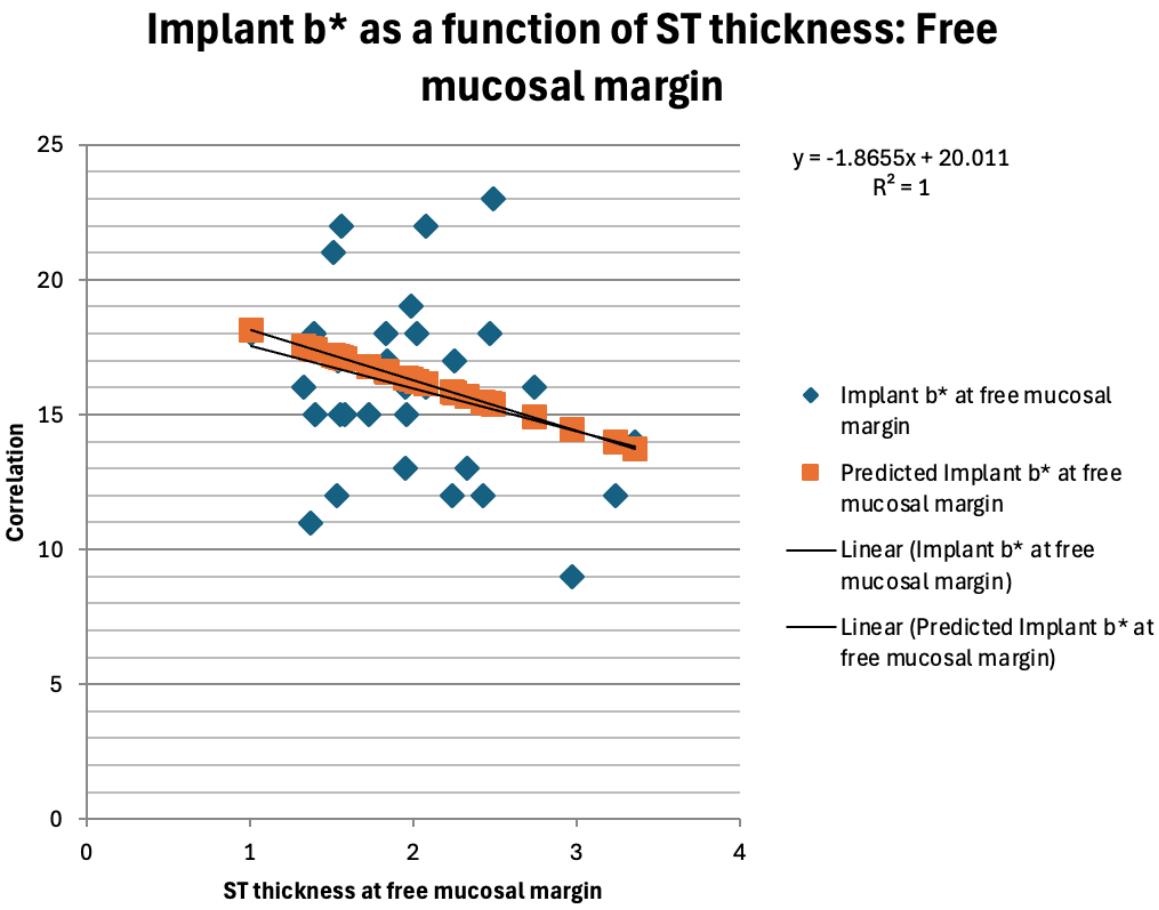

Figure 16: Linear regression analysis of scatter plot data, showing a negative relationship between implant b* value and thickness of the free mucosal margin.

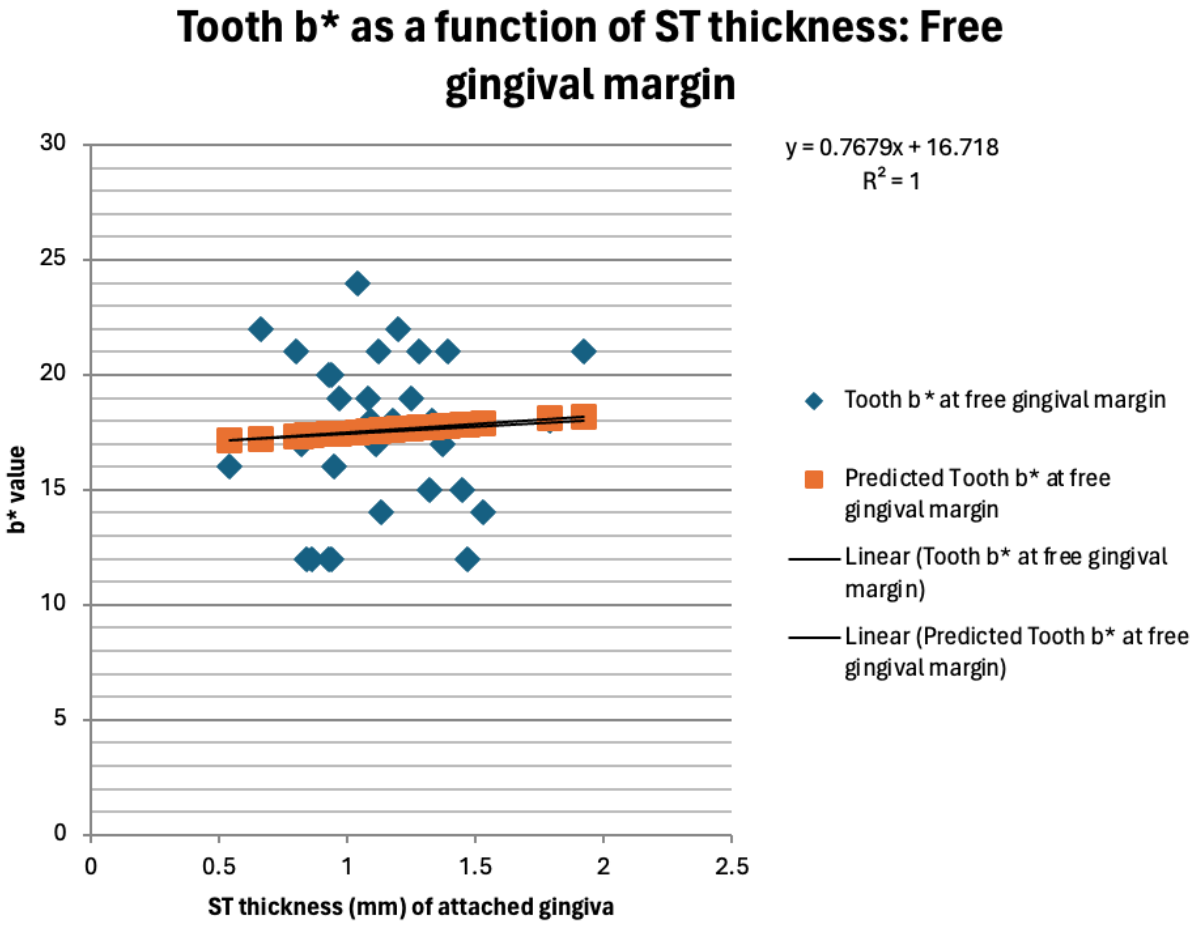

Figure 17: Linear regression analysis of scatter plot data, showing a positive relationship between tooth b* value and thickness of the free gingival margin.

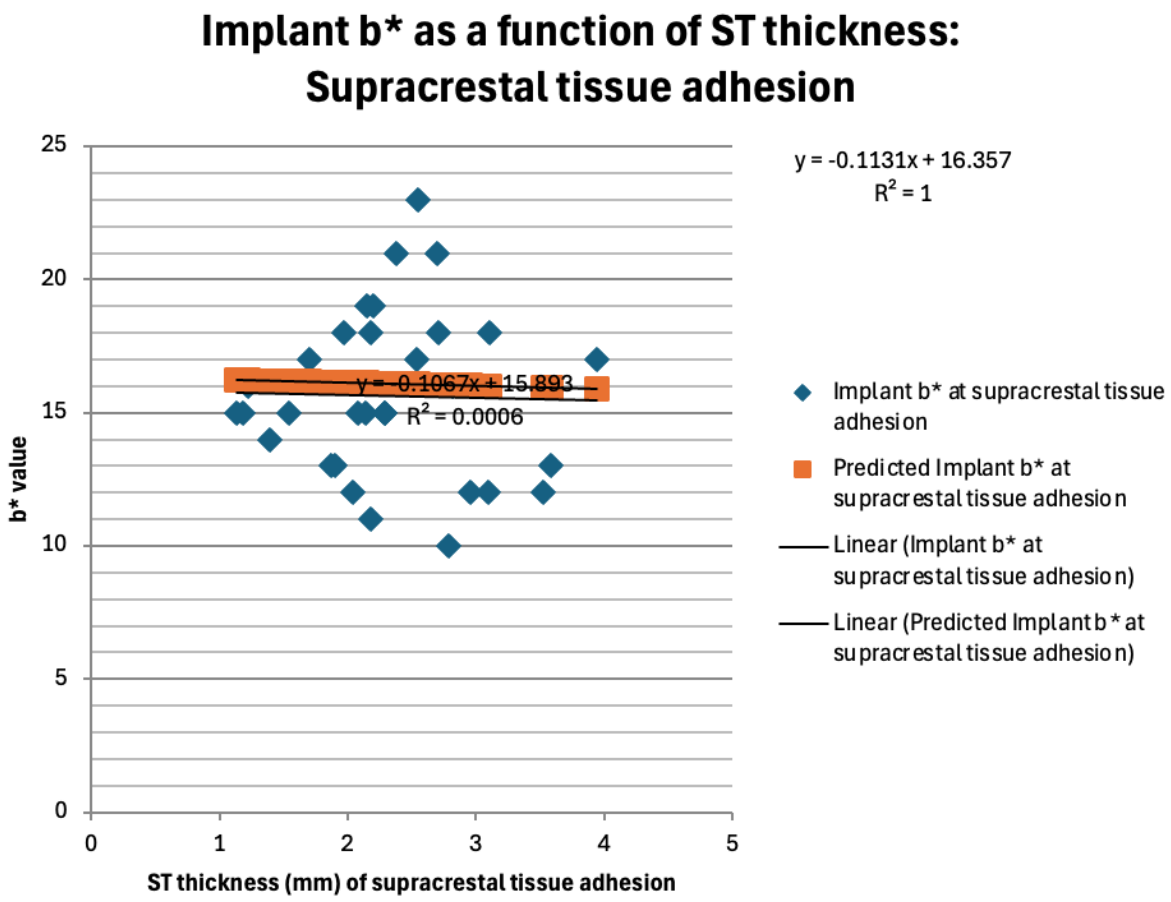

Figure 18: Linear regression analysis of scatter plot data, showing a weakly negative relationship between implant b* value and thickness of the supracrestal tissue adhesion.

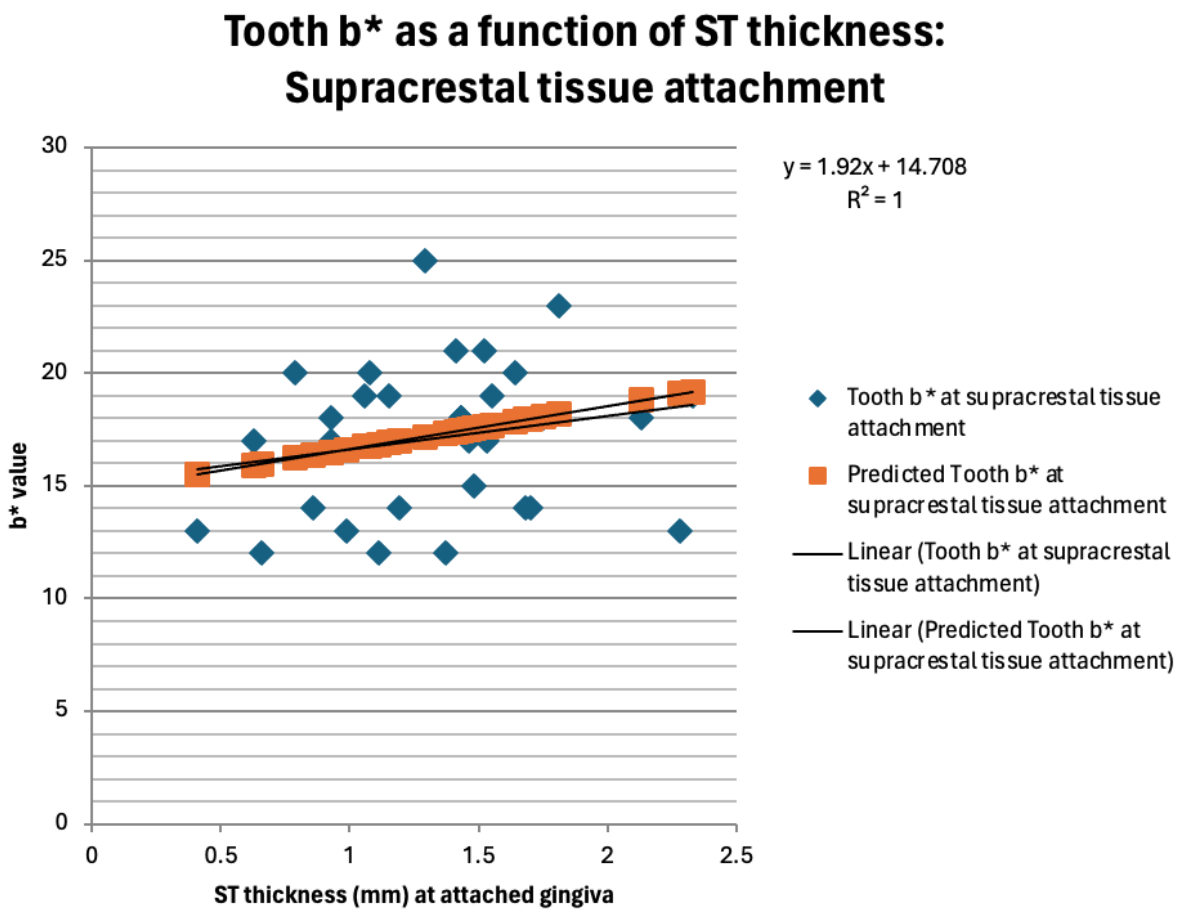

Figure 19: Linear regression analysis of scatter plot data, showing a weakly negative relationship between implant b* value and thickness of the supracrestal tissue adhesion.

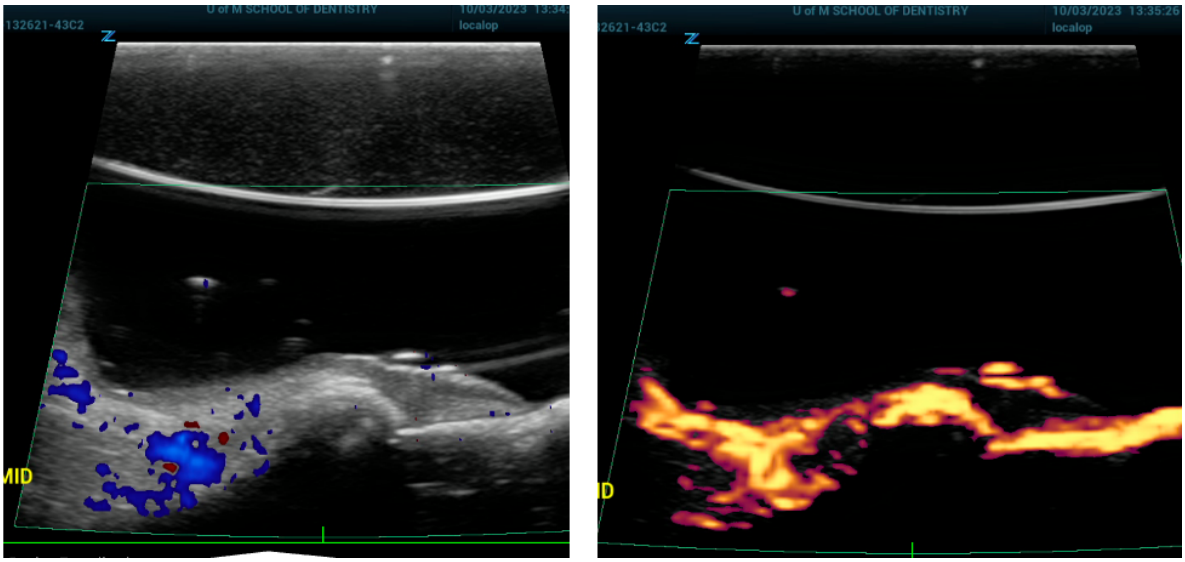

Figure 20: Left image: Natural tooth with perfusion analysis showing vascular flow within the buccal tissues. Right image: Power analysis showing the velocity of vascular flow of the same natural tooth.

	A	B	C	D	E	F	G	H	I	J	K	L	M	N	O
1	PHOTO DISTANCE MEASURES - IMPLANTS									PHOTO DISTANCE MEASURES - TEETH					
2	HMS #	M CEJ-CEJ	M PapH	M PapC	D CEJ-CEJ	D PapH	D PapC		HMS #	M CEJ-CEJ	M PapH	M PapC	D CEJ-CEJ	D PapH	D PapC
3	1	5.15	4.3	0.85	4.91	2.14	0.94		1	4.8	2.93	1.12	3.89	2.39	0.81
4	2	5.45	2.83	0	6.55	3.02	0		2	6.2	3.1	0	7.01	2.08	0
5	3	7.77	5.29	0	9.34	4.67	0		3	7.3	5.6	0	9.74	4.31	0
6	4	5.81	1.98	1.1	6.67	1.85	0		4	6.91	4.49	1.31	5.09	2.06	1.08
7	5	6	2.58	0	7.44	1.65	1.14		5	5.81	3.81	0	5.43	3.24	0
8	6	7.55	4.78	0.66	6.15	2.74	0		6	7.54	4.48	0.66	8.83	5.63	0
9	7	7.1	3.24	0	4.44	1.27	0		7	6.71	3.3	0	5.25	2.7	0
10	10	3.75	1.07	0	5.09	1.66	0		10	5.22	2.83	0.95	6.16	1.44	1.72
11	11	6.34	4.13	0	6.38	3.39	0		11	8.01	3.16	0	6.58	4.89	0
12	12	5.24	2.18	0	4.15	1.19	0		12	5.86	2.44	0	6.47	2.32	0
13	13	6.21	4.26	0	8.1	4.1	0		13	5.69	4.17	0	7.62	3.4	0
14	14	6.08	2.45	0	7.19	2.5	0		14	5.57	2.61	0	5.73	2.45	1.23
15	15	9.38	4.37	0	9.25	3.58	0		15	9.38	4.37	0	9.26	4.33	0
16	16	5.29	1.82	0	4.68	1.52	0		16	8.9	4.84	0	5.84	2.6	0
17	17	5.3	0.92	0	5.3	1.18	0		17	6.47	3.71	0	5.58	3.16	0
18	18	6.72	2.97	0	8.36	1.4	0		18	6.49	2.36	0	7.23	2.38	0
19	19	5.39	3.09	0	5.35	1.12	0		19	4.29	2.06	0	3.78	1.64	0
20	20	7.57	4.68	0	7.58	3.05	0		20	6.04	3.39	0	6.36	3.87	0
21	21	5.19	2.14	0	5.86	2.84	0		21	8.13	4.24	0	6.57	4.07	0
22	22	7.6	3.2	0	8.42	2.49	0		22	10.22	3.61	2.35	7.92	3.89	0
23	23	4.56	2.37	0	5.77	1.88	0.62		23	6.34	2.72	1.84	4.94	3.73	0.45
24	24	6.62	2.08	0	8.21	4.03	0		24	7.91	2.95	0	7.33	3.4	0
25	25	6.15	2.09	0	7.08	2.97	0		25	6.18	3.05	0	5.2	1.23	0
26	26	9.42	6.05	0	7.4	3.12	0		26	9.42	6.05	0	7.01	4.35	0
27	27	4.08	2.42	0	3.59	1.76	0		27	5.22	4	0	5.39	2.8	0
28	28	5.9	4.12	0	4.68	1.63	0		28	5.93	4.96	1.37	6.01	3.97	0
29	29	6.07	4.04	0.5	4.07	1.18	1.31		29	7.49	5.13	0	3.3	2.55	0
30	30	2.72	1.49	0	1.94	0.33	0		30	6.19	4.03	0	0	0	0
31	31	3.13	1.52	0	4.69	2.99	0		31	6.61	2.8	0	5.93	2.38	0
32	32	6.39	3.58	0	4.03	1.01	0		32	7.01	5.29	1.17	8.17	4.65	0
33	33	4.47	2.28	0	3.79	1.48	0		33	6.74	3.87	0	0	0	0
34	34	7.12	2.26	0	7.77	1.25	1.5		34	10.07	3.08	1.78	7.29	1.59	1.57
35	36	7.1	3.15	1.39	7.58	2.66	0		36	6.84	3.81	0.5	5.8	3.13	0
36	AVERAGES	6.0187879	3.0221212	0.1363636	6.1154545	2.2318182	0.1669697		AVERAGES	6.8936364	3.7345455	0.3954545	5.9609091	2.9281818	0.2078788
37	STD DEV	1.52502	1.2512787	0.3507387	1.8242997	1.042858	0.4188413		STD DEV	1.4646284	0.9947616	0.678238	2.1246946	1.3046682	0.4852561
38	TTEST 2 tailed	0.0011185	0.0012489	0.0382213	0.5836885	0.0021988	0.6542931								

Figure 21: Photoshop-based measurements. D -CEJ: Distal papilla base (aka, “papilla width”) measured from gingival zeniths of adjacent teeth. DPAP H: Height of the distal papilla as

measured from D CEJ-CEJ to the papilla tip. Similar measurement landmarks are used for M CEJ-CEJ, MPAP H height.

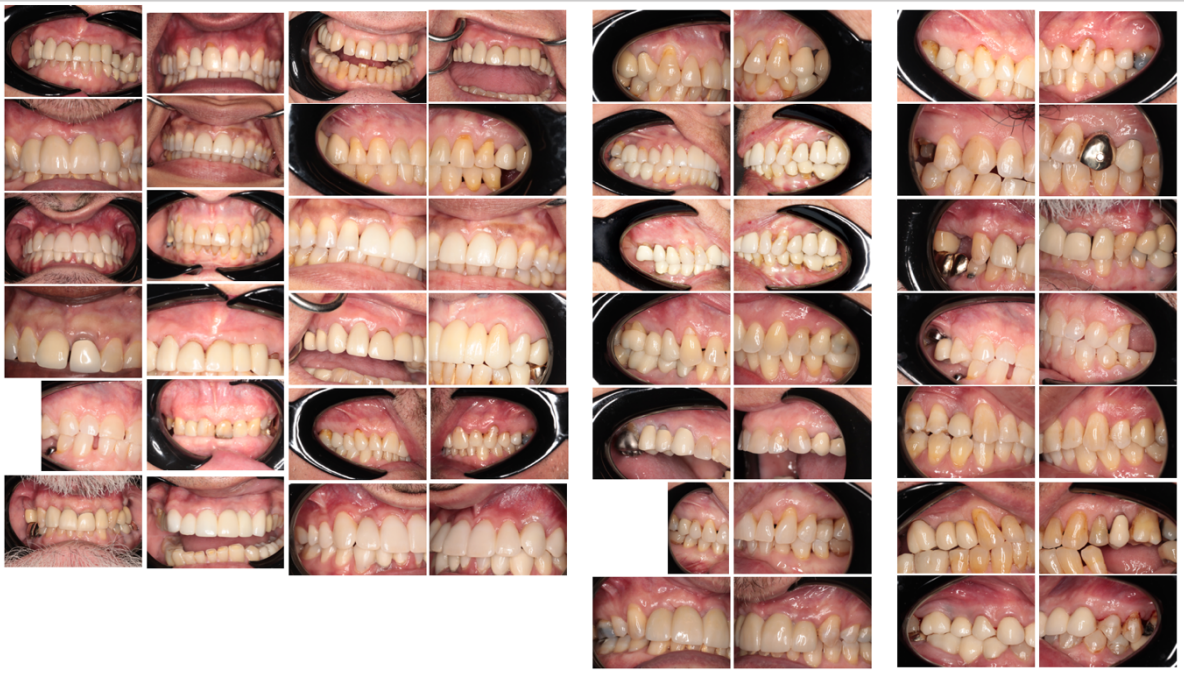

Figure 22: Clinical photo samples.

Patient #	Implant papilla ST thickness	Tooth papilla ST thickness
1	1.63	1.89
2	2.55	0.79
3	2.08	0.93
4	1.7	1.15
5	3.58	1.43
6	3.94	1.19
7	2.04	1.29
8	3.09	0.86
9	1.9	1.53
10	1.39	1.43
11	2.54	1.55
12	1.22	1.08
13	2.7	1.81
14	1.18	0.66
15	2.15	1.52
16	2.96	1.48
17	2.2	0.93
18	2.29	1.64
19	2.82	2.33
20	2.14	1.7
21	2.71	1.06
22	3.1	2.13
23	2.29	0.63
24	1.13	1.68
25	2.18	1.75
26	3.52	2.28
27	2.18	0.41
28	2.79	1.37
29	1.87	1.46
30	1.97	1.11
31	1.54	0.99
32	2.38	1.41
33	2.32	1.83
Average	2.30545455	1.37272727
Stdev	0.68788213	0.46673248
TTEST:	2.3876E-08	

Figure 23: Papilla thickness comparison between implants and natural teeth, obtained via ultrasonographic analysisExample of sagittal “slice” sections in Horos software.

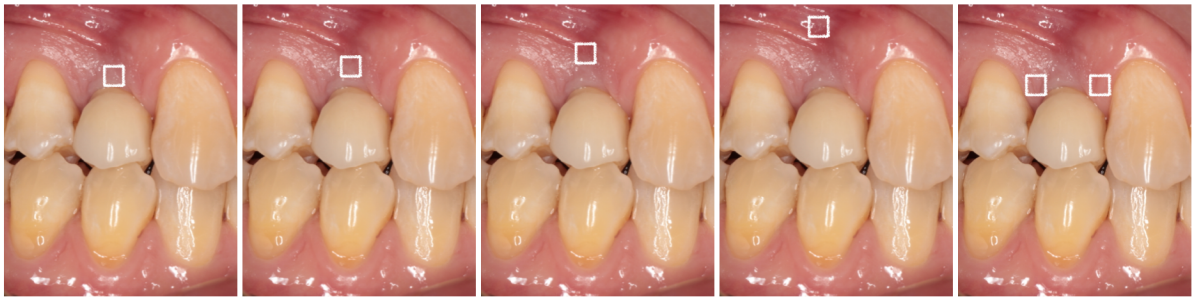

Figure 24: Color measurement zones. Each zone measured 2x2 mm. From left to right: Free mucosal margin, supracrestal tissue adhesion, MGJ, mucosa apical to MGJ, mesial and distal papillae.

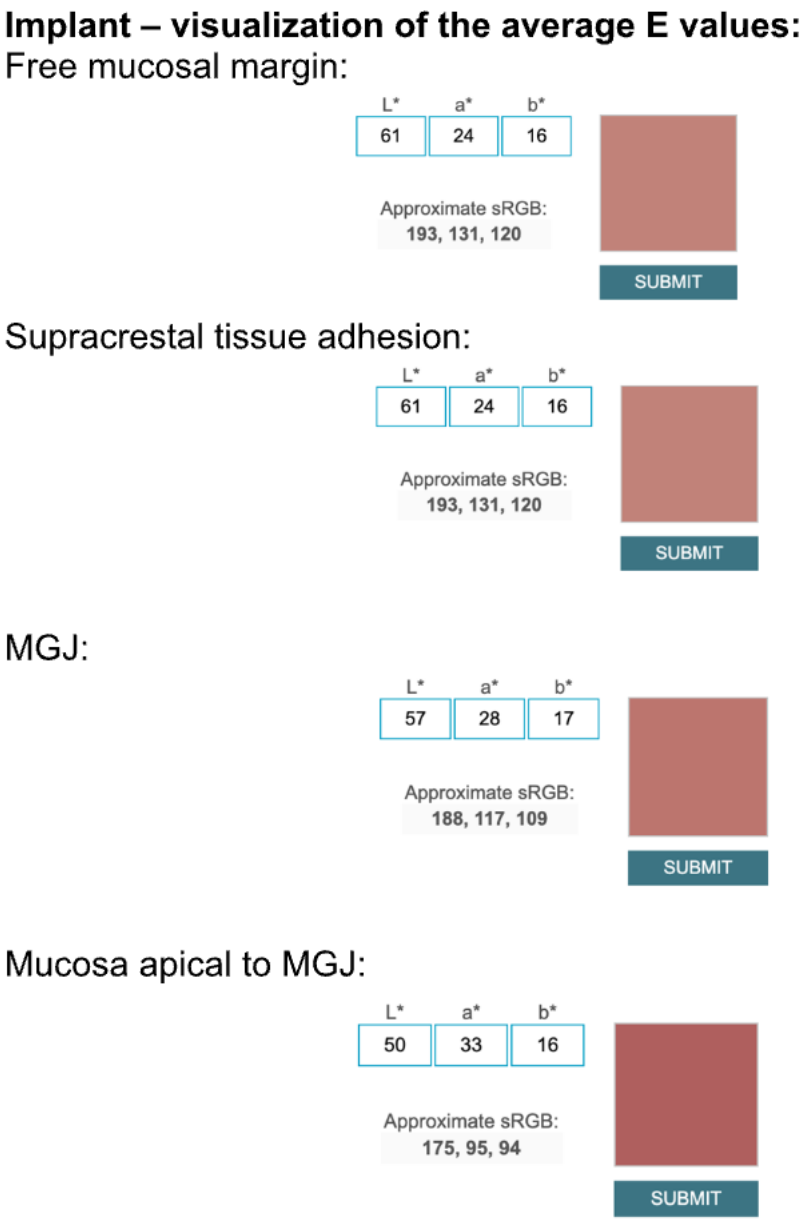

Figure 25: Visualization of the color averages of the different implant zones.

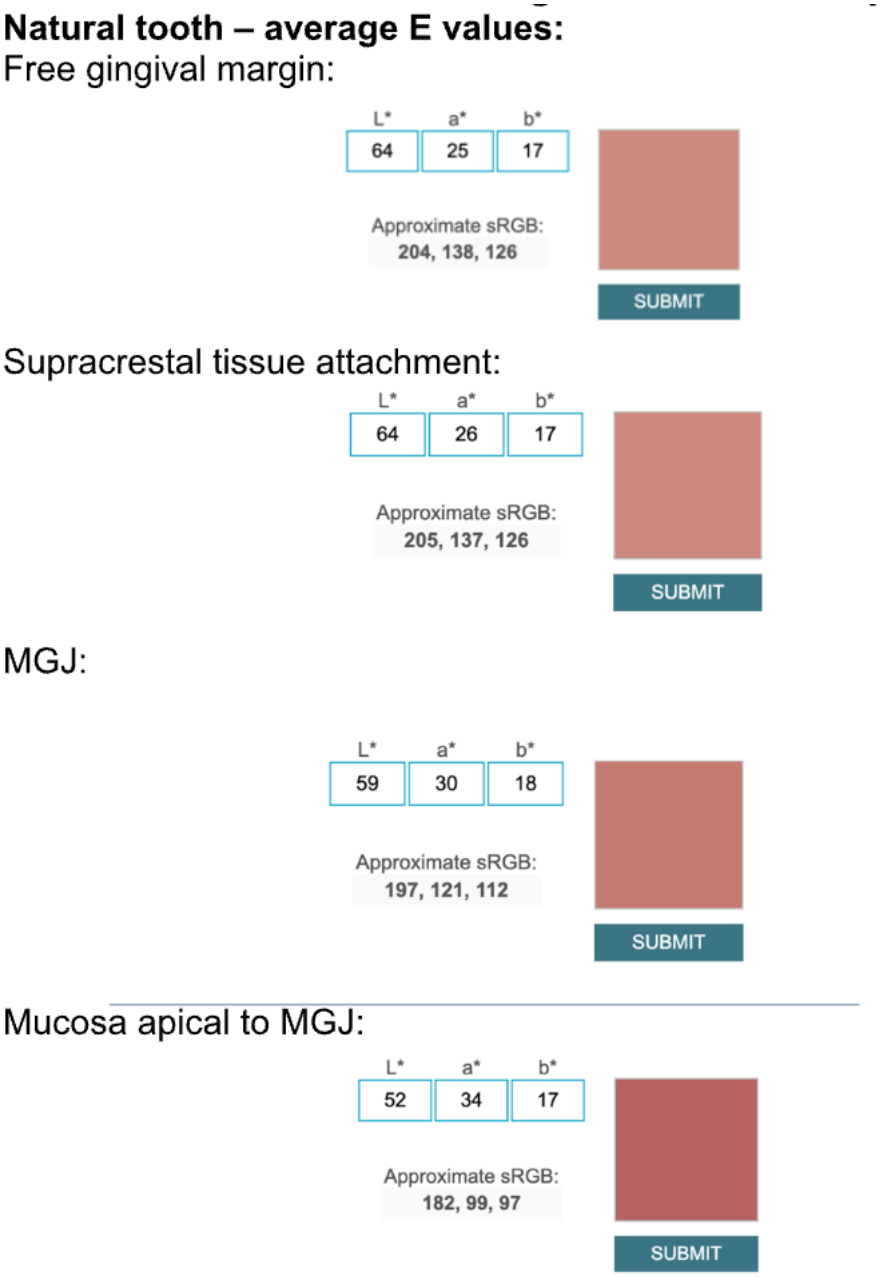

Figure 26: Visualization of the color averages of the different tooth zones.

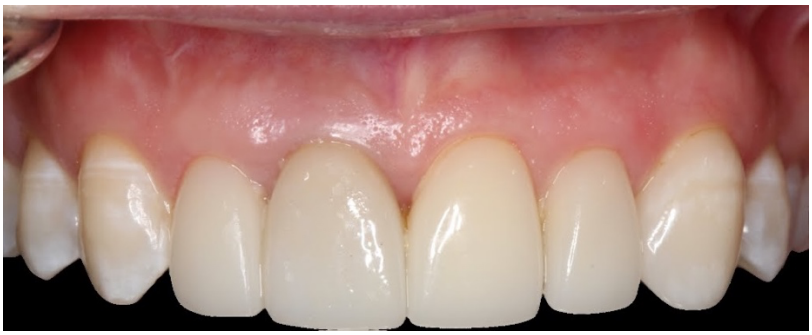

Figure 27: Implant exhibiting an implant-supported crown surrounded by healthy peri-implant mucosal tissues at the #8 site.